/

10P.

X64-36079

Code 2A - Cat. 09

THE JOHNS HOPKINS UNIVERSITY
DIELECTRICS LABORATORY

TR-15 Final Report
April 1, 1963 to June 30, 1964
Contract No. NAS8-5253
Control No. TP3-85286 (1F)
CPB-02-1130-63

THE JOHNS HOPKINS UNIVERSITY
DIELECTRICS LABORATORY
405 NORTH CAROLINE STREET
BALTIMORE 31, MARYLAND

Report:	TR-15 Final Report
Period:	April 1, 1963 to June 30, 1964
Contract No.:	NAS8-5253
Control No.:	TP3-85286 (1F) CPB-02-1130-63
Title:	Investigation of the Behavior of Dielectric Materials at High Field Strengths in a High Vacuum Environment
Prepared by:	Louis J. Frisco Research Contract Director
Date:	June 30, 1964
To:	National Aeronautics and Space Administration George C. Marshall Space Flight Center Huntsville, Alabama Attn: PR-EC

This report was prepared by The Johns Hopkins University, Dielectrics Laboratory under Contract NAS8-5253, Investigation of the Behavior of Dielectric Materials at High Field Strengths in a High Vacuum Environment, for the George C. Marshall Space Flight Center of the National Aeronautics and Space Administration. The work was administered under the technical direction of the Propulsion and Vehicle Engineering Division, Engineering Materials Branch of the George C. Marshall Space Flight Center with E. C. McKannan, Contracting Officer's Technical Representative, acting as project manager.

CONTENTS

Investigation of the Behavior of Dielectric Materials at High Field Strengths in a High Vacuum Environment

I. Mission Statement

The Contractor, as an independent Contractor and not as an agent of the Government, shall, during the term of this contract, utilize its best efforts and supply the necessary personnel, facilities, and materials (except those which may otherwise be provided), and do all things necessary for, or incident to the improvement of the basic understanding of breakdown in dielectric materials, and to provide useful engineering data, not presently available, on common dielectrics, with particular emphasis directed toward determining breakdown strengths at high frequencies.

Additional effort has been authorized to continue certain phases of previous investigation of the effects of space environment on the properties of dielectric materials. These studies are associated with the effects of a vacuum, x-ray irradiation and temperature on the a-c loss properties (ϵ' and $\tan\delta$) and the d-c conductivity of insulating materials.

II. Material Designations

The various materials that were used in this program are identified as follows:

Designation	Description and Supplier
TFE-6	Polytetrafluoroethylene extrusion resin, commercial designation TFE-6. E.I. du Pont de Nemours and Company, Wilmington, Delaware.
TFE-7	Polytetrafluoroethylene molding resin, commercial designation TFE-7. E.I. du Pont de Nemours and Company, Wilmington, Delaware.
FEP-100	Copolymer of tetrafluoroethylene and hexafluoropropylene, melt processable resin, commercial designation FEP-100. E.I. du Pont de Nemours and Company, Wilmington, Delaware.
PF	Polytetrafluoroethylene resin which had been stored in the laboratory for about 11 years. U.S. Gasket Company, Camden, New Jersey.
Mylar, Type C	Polyester, capacitor film, commercial designation MYLAR 130-100C. E.I. du Pont de Nemours and Company, Circleville, Ohio.
C-1147	Composition of methyl styrene with a small amount of dimethyl siloxane additive. Specimens supplied by the Delaware Research and Development Corporation, Wilmington, Delaware.
Styron-666	Polystyrene, commercial designation STYRON 666, unmodified molding compound. Dow Chemical Company, Midland, Michigan.
Alathon-10	Polyethylene, commercial designation ALATHON 10, injection molding resin. Medium density (crystallinity), narrow molecular weight distribution and low melt index. E.I. du Pont de Nemours and Company, Wilmington, Delaware.
K-4	Polychlorotrifluoroethylene, commercial designation KF-6050, ASTM- 1430-58T, Grade II, ZST 217, pelletized, injection molding and extrusion resin. Minnesota Mining and Manufacturing Corporation, St. Paul, Minnesota.

III. Factual Data

A. D-C Conductivity

A study of x-ray induced conductivity was in progress at the time that the present program was initiated. A detailed report of that study was presented in the Final Report of Contract DA-36-039-SC-89147[1]. In an environmental study it is necessary to be concerned with the instantaneous effects produced by a sudden change in environmental stress and the long-time effects of prolonged exposure to a fixed environmental stress. The instantaneous effects of irradiation on the d-c conductivity of organic materials has received a cnnsiderable amount of attention by several workers, and the relationship between induced conductivity and dose rate for very short exposure periods has been fully discussed by Fowler[2]. For exposure periods of less than one hour, the maximum values of induced conductivity, σ_m, follow the relationship $\sigma_m \propto R^{\Delta}$, where Δ is a constant that is characteristic of the material and R is the dose rate. With the 50-KVP x-rays used in this study, σ_m did follow the exponential relationship for polyethylene, polytetrafluoroethylene and polyethylene terephthalate.

For longer exposure periods the x-ray induced conductivity was found to vary with total absorbed dose and with dose rate. Polyethylene terephthalate, which was the only material that was examined at elevated temperatures, exhibited a complex behavior in the presence of the combined environmental stresses (radiation, temperature and vacuum). The purpose of continuing the investigation was to separate the effects of these environmental stresses so that the observed behavior could be better understood.

The experiments that have been conducted during this present program have been described in detail in the Quarterly Progress Reports. This phase of the investigation was devoted to dark conductivity measurements on Mylar Type C. A brief summary of the results is given below.

The first series of measurements were made in vacuum (10^{-6} torr range) at temperatures up to 130°C. The results of prolonged exposure are shown by the solid curves of Figure 1. In this series of measurements the specimens were preconditioned in the vacuum chamber at room temperature for 24 hours. They were heated and electrified at the same time, i.e., the

voltage was applied to the specimen at the same time that the heaters were energized. In all cases, the specimens were continuously electrified throughout the exposure period. Thermal equilibrium was reached in about 10 to 15 minutes, depending on the temperature. The behavior is somewhat erratic during the period before the specimen temperature stabilizes, so the data for this period are not shown. The spread in results from sample to sample was less than 15% which is remarkably low for conductivity measurements.

The steady decrease in conductivity at all temperatures in the range of 25 to 130°C suggests that vacuum exposure causes a continuous removal of products that contribute to the conduction process. When measurements were made at atmospheric pressure, however, the same steady decrease in conductivity was observed, as shown by the data (broken lines) of Figure 1. Therefore, it must be concluded that the vacuum exposure alone does not have any great effect on conductivity. The long-time decay is associated with the fact that the specimen is electrified during the entire experiment.

As mentioned above, each of the specimens was exposed to high vacuum for about 24 hours before being electrified and energized. During the early stages of electrification and heating the observed currents were large and it was difficult to make accurate measurements because the currents changed so rapidly. Such large transient currents are to be expected, but it is interesting to note that in another series of measurements, where the specimens were electrified for 23 hours before the heaters were energized, even larger transients were observed. Furthermore, as shown in Figure 2, these transients decay at a slower rate than those observed in the previous experiments. This comparison is shown by the curves of Figure 2. The decay is more rapid at 66°C than at 43°C and it is expected that it would be even more rapid at higher temperatures.

It is rather surprising that the specimens that were electrified before heating exhibited such large and slowly decaying transients that are normally observed during the early stages of electrification had decayed before the heaters were energized; the conductivity of these specimens was in the 10^{-20} mho cm^{-1} range at the beginning of the heating period. Therefore, it was not expected that the transients caused by heating alone would be so large and last so long. Although this effect is not understood, it is noteworthy because it indicates the magnitude of changes in conductivity that can occur during temperature cycling.

Measurements of conductivity that were made in the course of studying the effects of prolonged vacuum exposure at elevated temperatures automatically provided information on the relationship between conductivity, σ, and absolute temperature, T. For a single conduction process the relationship $\sigma = \sigma_o e^{-W/kT}$ should hold, where W is the activation energy of the conduction process and k is Boltzmann's Constant. Therefore, a plot of "log σ vs 1/T" should result in a straight line with a slope of -W/k. When such an analysis was made using the values of σ that were observed after equal periods of exposure at each temperature, the resulting curves (one for each time period) had different slopes above and below the glass transition region (70 to 80°C). In each case the slope, and, therefore, the activation energy was higher at temperatures above the glass transition region.

Because the experiments that provided these data were designed for the purpose of studying the effects of vacuum exposure at various temperatures, each specimen was held at a fixed temperature during the entire exposure period. It can be seen from the data of Figure 1 that conductivity steadily decreased at all temperatures as the exposure period was prolonged. Therefore, the "log σ vs 1/T" curves did not indicate true values of activation energy. The points on each curve were taken from different specimens, each with a different exposure history.

To determine the true relationship between conductivity and temperature, measurements were made on specimens that were conditioned in vacuum at elevated temperatures (120-130°C) for 150 hours and then allowed to cool at a controlled rate. To eliminate the transient current that accompanies a change in temperature, the temperature was lowered in increments and held constant at each step until the transient had decayed. At temperatures below the glass transition region, the decay period was at least two hours. Shorter periods of 15 to 30 minutes were sufficient at temperatures above the glass transition range. Only a limited number of measurements were made at temperatures below 40°C because of the long time required for the transients to decay.

The results of these measurements are summarized in the log σ vs 1/T curves shown in Figure 3. Typical data are given for measurements in

vacuum at 180 and 320 volts. Both curves have higher slopes at temperatures above the glass transition region. This suggests that there are at least two conduction processes and that the high-temperature conduction process has a higher activation energy. It might be expected, for instance, that a process such as ion transport in the amorphous region would be radically affected as the temperature was raised above the glass transition point, while a process associated with the crystalline phase would not be significantly altered at temperatures below the crystal melting temperature. During these experiments it was found that a specimen that had been slowly cooled from 130°C to 25°C could be slowly reheated in a manner that produced the same values of conductivity as those observed during the cooling cycle. Therefore, the 150 hour preconditioning at 130°C had been sufficiently long to provide values of conductivity that remained essentially unchanged during the period required for the measurements.

The high temperature data agree with the results reported by Amborski[3], who found that for crystallized and oriented polyethylene terephthalate the activation energy of the conduction process was about 1.8 eV in the temperature range of 100 to 200°C.

The data shown in Figure 3 indicate that there is a slight difference in conductivity as the voltage is increased from 180 to 320 volts. Each of these curves, however, represents the behavior of a particular specimen that was electrified at a fixed voltage. Additional data was required to determine the effect of applied voltage on conductivity.

A final series of measurements was conducted to clarify the dependence of dark conductivity on applied voltage and temperature. Each specimen was electrified and heated at 130°C for about 150 hours in vacuum before the measurements were begun. This preconditioning eliminates significant changes due to aging during the remainder of the experiment. Two test methods were employed:

(1) The voltage was held constant while the temperature was successively lowered to prescribed values over the desired range. Measurements were made at each temperature after sufficient time was allowed for the transient

current to decay. After each series of measurements was completed, the temperature was increased to 130°C, the voltage was adjusted to a new value and the procedure was repeated.

(2) Starting at the highest temperature, measurements were made at each desired voltage, allowing sufficient time at each voltage for transient currents to decay. The temperature was then decreased to a new value and the procedure was repeated.

A complete set of measurements on a single specimen takes from 2 to 3 weeks because of the long preconditioning period and the long decay times of the transients caused by changes in voltage or temperature. Although equilibrium can be reached in a matter of minutes at the higher temperatures, much longer times are required at the lower temperatures. At 80°C, for instance, a whole day is required for the transient to decay after making a change in the applied voltage.

The results obtained using both test methods are summarized in Figures 4 and 5. Each curve represents the average behavior of seven specimens. At lower temperatures, where the spread in results is greater, the long time required for transients to decay made it impractical to extend the measurements to temperatures below 70°C.

Figure 4 shows that log σ is a linear function of voltage, or that $\sigma \propto k\, e^{mV}$, where k is dependent on temperature and m is approximately 0.0025 $volt^{-1}$ at all temperatures in the range from 70 to 130°C.

This result differs slightly from that of Amborski[3], who found a hyperbolic sine relationship ($I = s' \sinh AV$) between current and voltage. The main difference occurs at the lower voltages where the hyperbolic sine function decreases more rapidly than the single exponential function. In his analysis, Amborski concludes from the observed current-voltage relationship that the conduction is ionic.

Time did not permit a study of the voltage effect at temperatures below the glass-transition region. At these lower temperatures the currents are so small and the transients decay so slowly that it is extremely time-consuming to fully investigate the voltage and temperature dependence of the conduction process. Because data was not obtained at temperatures below 70°C, the curves of Figure 5 do not show the change in activation energy at temperatures below the glass transition region.

B. Radiation Induced A-C Losses

1. Previous Investigation

In a previous program[1], measurements of dielectric constant and tanδ were made on several materials during 50 KVP x-ray irradiation in high-vacuum. The largest effects were those exhibited by TFE-6 and TFE-7. Briefly, the previous results on these fluorocarbon polymers can be summarized as follows:

(a) Both TFE-6 and TFE-7 exhibited large increases in dielectric constant and tanδ during x-ray irradiation in high-vacuum. Typical results for TFE-7 are shown in Figures 6 and 7. The increase in tanδ to a maximum value, followed by a steady decrease during the remainder of the x-ray exposure period was a reproducible effect that was observed in every case.

(b) When the irradiation was discontinued, the induced losses decayed to relatively low values, as shown in Figure 8. The low value was maintained as long as the specimen was kept in a high-vacuum. When the cell was vented to the atmosphere or filled with dry (oil pumped) nitrogen, the losses immediately increased and then slowly decayed for long periods of time (several months in some cases).

(c) Diffusion had no effect on induced losses, as demonstrated by results on specimens of different thickness.

(d) The presence of oxygen during the sintering process did influence the effects of irradiation in vacuum. Specimens

sintered in nitrogen, rather than air, exhibited smaller induced losses during the early stages of exposure, but considerably higher losses during the latter stages (5 to 16 megarads).

(e) The x-ray induced losses decreased rapidly with increasing frequency.

(f) The permanent losses (those that persisted after many days of recovery) appeared to be voltage dependent. The low frequency tanδ decreased with increasing voltage.

These results could not be explained on the basis of well known effects of radiation on tetrafluoroethylene polymers. However, they did suggest several experiments that might provide significant information on the nature of the induced loss mechanism. Some of these experiments were conducted in the present program. The significant results are summarized in the following sections.

2. Procedures

A Machlett AEG-50 tube capable of continuous operation at voltages up to 50 KVP and anode currents up to 50 ma was used as a source of x-rays. Radiation was introduced into a vacuum chamber through a beryllium window identical to the one in the tube.

A three-electrode specimen holder with heaters and a temperature control circuit was designed to facilitate the measurement of induced losses at elevated temperatures. The holder was placed in a vacuum chamber. Measurements of dielectric constant and dissipation factor were made with a General Radio 1610-B Capacitance Measuring Assembly.

To reduce the time required for each x-ray exposure experiment, the dose rate was increased from 0.025 megarads/hr, which had been used previously, to 0.2 megarads per hour. A comparison of the typical results obtained at these two dose rates is given in Figure 9. The nature of the effects remained the same, but the peak value of tanδ occurred at a higher absorbed dose when the higher dose rate was used. It is not surprising that the induced losses, which are associated with at least two time-dependent

processes, should be dose-rate dependent. On a time comparison, the peak value of tanδ occurred much earlier in the exposure period when the higher dose rate was used. The results showed that the effects could be studied using the higher dose rate, thereby saving a great deal of time.

3. Effect of Temperature

To determine the effect of temperature on x-ray induced losses a series of experiments was conducted in which the specimens were maintained at various fixed temperatures up to 158°C during irradiation in vacuum. The specimens were preconditioned in vacuum at the prescribed test temperature for 24-hours.

The effect of temperature, as shown in Figure 10, is striking. The large transient effect at 28°C was greatly moderated at 158°C, but it was amplified at the intermediate temperature of 89°C. Similar results were, of course, obtained in the dielectric constant measurements. In addition to affecting the rate at which the interactions occurred, the increased temperature caused the specimens to be more completely degassed. Now, it was known from previous experiments that the induced losses remained high during the entire exposure period if the irradiation was carried out in air at atmospheric pressure, or conversely, that the losses reached a peak value and then steadily decreased if the irradiation was carried out in vacuum. Therefore, the results of Figure 10 suggested that the moderating effect could be caused by the more effective removal of gases from the specimen and the cell at the elevated temperatures.

To determine if degassing of the specimen and walls of the vacuum chamber was responsible for the observed temperature effect, measurements were made on specimens that were baked in vacuum at 160°C for at least 72 hours and then allowed to cool to room temperature in vacuum before radiation was introduced. The moderating effect of this bake-out is shown by the data of Figure 11. The maximum values of tanδ and dielectric constant for the baked-out specimens were considerably less than the corresponding values for specimens that were not baked. However, the radiation effects were still considerably greater than those observed in the high temperature experiments (Figure 10).

It was felt that more complete degassing would further reduce the induced losses. Significant quantities of gas could leak into the vacuum chamber during the period required for cooling the specimen and during the irradiation period. Because the specimen was mounted in a relatively large vacuum chamber, it took approximately 12 hours to cool from 160°C to room temperature. Another experiment was conducted in which the vacuum chamber was filled with helium during the cooling period. The increased heat transfer reduced the cooling period to about one hour. The chamber was then evacuated before the radiation was introduced. The effects of this rapid cooling with helium are shown in Figure 11. Tanδ rapidly reached a peak value, even higher than that exhibited by the unbaked specimen, but then decayed rapidly to a value lower than that exhibited by the slowly cooled or the unbaked specimens. Again, similar results were obtained in the dielectric constant measurements.

The sharp transient exhibited by the helium cooled specimen is not understood, but it is interesting to note that it occurred at an absorbed dose of about 0.15 megarads, which is in the dose range where smaller peaks occurred in many of the other experiments. In spite of this unexplained peak, the results show that degassing greatly influences the results of experiments at elevated temperatures. Other workers have shown that degassing reduces the effect of gamma radiation on the mechanical properties of polytetrafluoroethylene[4].

4. Recovery Effects

Typical recovery data for TFE-7 are shown in Figure 8. Without exception, the induced losses decayed rapidly when the irradiation was removed, and then maintained a steady value as long as the specimens remained in vacuum. However, when the cell was filled with air or dry nitrogen (oil-pumped) an immediate increase in tanδ occurred and the subsequent slow decay continued for many months.

During the present program experiments were conducted to determine if an inert gas, such as helium, would influence the recovery behavior. It was found that after 24 hours of vacuum recovery, filling the vacuum cell with helium caused no detectable changes in tanδ, which had stabilized at a value of 0.0002. After four hours the helium had caused no change in tanδ, so the cell was evacuated and then filled with dry nitrogen. The 100 cps tanδ

then increased rapidly, reaching a value of 0.0012 in five minutes, 0.016 in one hour and 0.1 in 24 hours. In a subsequent experiment a specimen was allowed to recover in the helium atmosphere for 72 hours and this caused the 100 cps tanδ to reach a value of 0.044. This slow change could have been caused by air leaking into the chamber.

The recovery experiments demonstrate the existence of radiation induced radicals that persist for relatively long periods in vacuum. It is well known that the presence of oxygen influences the effects of radiation on the properties of TFE materials. It would be expected, therefore, that the reaction that occurs when the chamber is filled with air involves the combination of oxygen and the radicals produced by the radiation. Water vapor could also play an important role. In the case of the reaction with dry nitrogen, there is some question concerning the amount of oxygen that was present as an impurity. The striking difference in behavior in nitrogen and in helium suggested that an experiment using more highly purified nitrogen would be justified. Time did not permit this experiment to be conducted.

5. Comparative Data for Other Fluorocarbons

In the previous programs, fluorocarbon materials other than TFE-6 and TFE-7 were examined but appeared to be unaffected by the x-ray irradiation. It did not seem reasonable, however, that materials such as FEP-100 and PF (see Page 2 for description) should exhibit none of the radiation effects that were so striking in the case of the other TFE materials. Therefore, these materials were re-examined in the present program where they could be irradiated at a higher dose rate and the loss properties could be measured with more sensitive equipment.

The detailed results for TFE-7, FEP-100 and PF are given in Tables I to V. The 100 cps tanδ data are summarized in Figure 12. It is now clear that the x-ray induced losses in FEP and PF were just below the limit of detection at the maximum absorbed doses in the earlier experiments.

The losses in FEP increase at a slower rate than those in TFE-7 and then go through a broad maximum. As the exposure is prolonged, however, the FEP losses decrease in a manner similar to that of the TFE-7 losses. It can be seen that for large doses the induced losses are not greatly different for the two materials.

It is interesting to note that the steady increase in tanδ exhibited by PF is similar to the behavior of TFE specimens that were sintered in the absence of oxygen (in nitrogen). This suggests that these old specimens of PF were taken from material that was not sintered in the presence of oxygen.

The absence of a sharp peak in the FEP data (Figure 12) suggests that residual gases in the vacuum chamber have less effect than they did in the case of the TFE materials. This observation is also in agreement with the recovery data of Table III which indicate that no appreciable change occurred when the vacuum cell was vented to the atmosphere. The obvious experiment suggested by these results is to irradiate FEP in air, but time did not permit this to be done.

A monochlorotrifluoroethylene polymer, designated K-4 (see Page 2 for description) which had been examined in the previous program was also included in the present study at the higher dose rate. The results of these measurements are summarized in Table VI. The initial losses in this material are, of course, much higher than those of the TFE materials, but they remain essentially the same throughout the exposure and recovery periods. The data show a slight decrease in tanδ at the lower frequencies that was also observed in the previous program.

Time did not permit the study of these other fluorocarbon materials to include exposure at atmospheric pressure or exposure at elevated temperatures in vacuum.

6. Effect of Voltage on Induced Losses

In the previous program electric strength measurements were made at 60 cps on TFE specimens that exhibited high dissipation factors as the result of x-ray irradiation. The stresses that those breakdown specimens

were capable of withstanding were much too high for a material with such a high tanδ (greater than 0.1). Thermal effects should have become evident at voltages much lower than the highest voltages that were applied. The absence of significant thermal effects suggested that the induced losses were decreasing with increasing stress. Such an effect, which is called the Garton effect for composite materials[5], can occur when the loss mechanism involves hindered ionic motion. In the case of the TFE polymers, the ions produced by the irradiation are apparently hindered by the polycrystalline phase of the polymer and they can only contribute to the loss during a part of each cycle of applied voltage. As the voltage is increased, the ions are only capable of moving during a smaller fraction of the period.

During the present investigation additional measurements were made on TFE-7 specimens both during and after x-ray irradiation. The results, although still qualitative, clearly showed that the induced losses steadily decreased as the applied stress was increased from 60 to 1000 VPM. These experiments substantiate the previous results and also establish the existence of a voltage dependence during irradiation and before the specimens are exposed to oxygen.

7. Induced D-C Conductivity

It has been shown that x-ray induced losses in TFE and FEP materials decrease rapidly with increasing frequency and that these losses also are voltage dependent. Both of these effects suggest the existence of an induced conduction mechanism. Adequate measurements of induced d-c conductivity during long-time exposure could not be scheduled in the previous program, but it was possible to initiate such a study in the latter part of the present program.

The general remarks that were made in the discussion of the conductivity of polyethylene terephthalate (Section III, A) also apply to the short-time behavior that would be expected in the case of the fluorocarbon materials. It is the long-time effects, however, that are of primary interest in this present study. In particular, the measurements were intended to determine if the d-c conductivity followed the same general behavior as the a-c losses during the exposure and recovery experiments.

A summary of the exposure data is given in Figure 13. These results were obtained on three specimens that received different pre-irradiation treatment. Specimen A was merely placed in the vacuum chamber at room temperature for 144 hours before irradiation. Specimen B was heated to 165°C in vacuum for 120 hours and then allowed to cool to room temperature over a period of 9 hours. Specimen C was heated at 166°C in vacuum for 117 hours and then rapidly cooled to room temperature by temporarily filling the chamber with helium. In all cases the specimens were in a vacuum environment during irradiation. Similar pre-irradiation treatments had significant effects on induced a-c losses, as shown in the discussion of temperature effects (Page 11).

All of the specimens exhibited a maximum value of induced conductivity during the early stages of exposure, followed by a steady decrease as the exposure period was extended. As previously reported, a-c losses exhibit the same transient behavior during x-ray irradiation.

Specimen C, which was degassed more thoroughly than the other specimens, exhibited the smallest induced conductivity. Again, this is in agreement with the effect of residual gases on the a-c behavior.

The recovery data are shown in Figure 14 for specimen A and in Figure 15 for specimens B and C. During recovery in vacuum, a steady decrease in conductivity was exhibited by each of the specimens. Specimen A was permitted to remain in the vacuum chamber for a longer period than the other specimens, but it showed little improvement after the first 24 hours. The initial conductivity of TFE-7 was less than 7×10^{-21} mho cm^{-1}, so the value of 1.6×10^{-19} mho cm^{-1} after 250 hours of recovery represented a significant permanent increase. Again, a permanent increase was also observed in the case of a-c loss properties.

Specimens B and C showed the same recovery characteristic as specimen A during the first 24 hour period in vacuum. At the end of the 24 hour recovery period in vacuum, specimen B was exposed to air at atmospheric pressure, and specimen C was exposed to helium at atmospheric pressure. In both cases, while the pressure was being increased it was

necessary to remove the test voltage (320 V.) so that gaseous ionization could be avoided. Except for this brief period, the voltage applied to a specimen remained unchanged during the entire exposure and recovery periods.

In both cases the specimens showed an immediate increase in conductivity when the pressure in the chamber was increased to one atmosphere. As shown in Figure 15, specimen B showed a larger initial increase in air than specimen C did in helium. In the case of a-c losses, an immediate increase was always observed when the cell was filled with nitrogen (oil-pumped) or air, but no large increase occurred during the early stages of recovery in helium.

The steady increase in conductivity of specimen C during the latter part of the recovery period may have been caused by leakage of air and water vapor into the helium-filled cell. A slow increase of this kind was also observed in the corresponding experiment on a-c losses.

The data certainly show that the pattern of behavior is the same for induced d-c conductivity and induced a-c losses. However, two effects show that the a-c losses are not caused by a simple conduction mechanism. First, the d-c conductivity was too small to account for more than 10% of the a-c losses. Second, the maximum value of tanδ usually occurred at an absorbed dose of 1 to 2 megarads, whereas the maximum value of conductivity occurred at about 0.15 megarads. However, neither of these effects is inconsistent with the behavior that might be exhibited by a hindered ionic conduction.

The combined data on dielectric constant, tanδ and d-c conductivity suggest the existence of both an induced ionic conductivity, which is hindered by the partially crystalline structure of the TFE polymer, and a dipole moment, which has a relatively long relaxation time (effect decays rapidly with increasing frequency above 100 cps).

In the case of the other fluorocarbon materials, induced d-c conductivity also followed the same general pattern as the a-c losses. The results of measurements on TFE-7, PF, FEP and K-4 are summarized in Figure 16.

In the case of the monochlorotrifluoroethylene resin, K-4, the irradiation was continued until a dose of 33 megarads had been absorbed, but no further increase in conductivity was observed.

C. Electric Strength Measurements

In a previous program[1] an improved breakdown specimen was developed for use in electric strength measurements over the frequency range from 60 cps to 18 mc. Only a few preliminary measurements had been made in that program, however, so the performance of the specimen was not fully evaluated. During this present reporting period a considerable amount of effort has been directed toward the determination of electric strength of polystyrene, using the improved specimen.

A cross-sectional view of the specimen is shown in Figure 17. The important feature of this specimen is the shape of the cavity. The thinnest section is located at the base of the circular groove. Therefore, the raised section at the center of the cavity, where machining is most difficult, is not involved in the breakdown. The tubular high-voltage electrode makes contact with an evaporated silver coating in the cavity, but does not rest on the bottom of the circular groove. To be sure that good contact is made, continuity between the raised section of the cavity and the tubular electrode is checked with an ohmmeter. In addition, contact is made between the tubular high-voltage electrode and the center of the raised section of the cavity which was painted with silver paint before the silver coating was evaporated. A silvered area on the bottom of the specimen is placed in contact with a ground electrode.

The specimen is fabricated from a 1/2" x 1 3/4" x 1 3/4" block. The cavity is started with a 3/4" diameter drill and then finished with a special tool in a lathe. The tool has a semi-circular tip (1/8" radius) which forms the groove at the base of the cavity. The specimen is mounted on a precision-ground backing plate that is held in the lathe chuck. A countersunk hole in each corner of the specimen permits machine screws to be used in mounting the specimen on the backing plate. This plate, which extends beyond the edges of the specimen, is used as a reference point in determining the depth of penetration of the tool to obtain a given thickness at the base of the cavity.

In all tests the specimen is immersed in transformer oil to eliminate corona in the vicinity of the electrodes.

The first series of measurements included tests at 2 mc on a group of 24 polystyrene specimens. The breakdown thickness at the base of the cavity was 10 mils in each case. The 2 mc voltage was raised manually until breakdown occurred. In this group of 24 specimens, 14 of the 24 failures occurred at stresses between 1.6 and 1.8 KV/mil, while 18 of the 24 failures occurred at stresses between 1.5 and 1.9 KV/mil. The median value was 1.7 KV/mil. The maximum and minimum values were 2.0 and 1.0 KV/mil respectively.

To determine if the thickness of the evaporated silver coatings influenced the results, a record of the estimated thickness of the coatings on each sample was made. Thickness variation was estimated by weighing the samples before and after the silver was deposited. The weight of silver in the recessed cavity varied from 1.1 to 3.4 mg., while that of the plane circular pattern varied from 1.8 to 7.0 mg. No correlation was found between the weight of deposited silver and the observed values of electric strength.

To reduce the temperature rise on the coated surfaces of the specimen, the silver was evaporated in 3-second bursts. The specimen was allowed to cool between bursts. It was determined that the energy measured transferred to the specimen surface by the hot silver was twice as much as that transferred by direct radiation from the crucible. The total heat flux on the recessed and plane surfaces was 1.5 and 9.0 watts respectively and, although the exposure occurs only during 3-second intervals, the increase in surface temperature could cause a change in the surface texture. To determine if the heat transferred during the evaporation process influenced the electric strength values, a second group of 25 specimens was prepared by a method that exposed the specimen surfaces to a higher heat flux and a higher total amount of transferred energy. This was done by permitting radiation from the empty crucible to heat the specimen. The results obtained on this group of specimens did not differ significantly from those obtained on the first group.

Although the spread in results for these tests at 2 mc is not unusual for breakdown measurements, the effect of voltage application time is a matter of serious concern. In most short-time breakdown tests, the voltage is linearly increased from zero to breakdown over a period of approximately 40 seconds. At low frequencies, where most electric strength testing is done, it is not difficult to obtain a test voltage that increases at prescribed rate. In the r-f range this is experimentally more difficult, particularly when the stresses are as high as those obtained with polystyrene. The high currents cause components of the tuned circuit to become heated and the resulting dimensional changes detune the circuit. Retuning can be accomplished within a few seconds, but during this period the specimen is subjected to a high stress. Consequently, breakdown will frequently occur during the retuning process or as soon as the voltage is increased after retuning. To determine the extent to which the time of voltage application influences the observed values of electric strength, a series of tests was conducted in which a constant voltage was applied and the time to breakdown recorded. The detailed results of these tests are given in Table VII.

Several significant observations can be made from this limited amount of data. In the r-f range, the time to failure decreases rapidly as the applied stress is increased. Furthermore, the character of failure changed from a highly localized puncture at the high-stress, short-time condition, to a general deformation of the critical volume at the low-stress, long-time condition. The deformation was caused by dielectric heating in the volume where the stress is greatest. This type of failure has been encountered in previous investigations with lossy materials. In the present experiments, the thermal conditions are more severe because of the small mass of the electrodes, and the stresses are considerably higher because of the reduced thickness (10 mils instead of 30 mils). Therefore, the pure thermal failure can occur even with a low-loss material such as polystyrene. It should be noted, however, that at 2 mc a stress of 1.0 KV/mil caused deformation after 15 seconds, but a stress of 1.7 KV/mil resulted in a pin-point

puncture after 3 seconds, with no evidence of significant heating, or deformation, outside of the failure site. The same pattern of behavior was observed at 5 mc and at 18 mc.

The 60 cps results, which are based on only one specimen, indicate that closer examination is required to determine if microscopic discharges at the high voltage electrode are causing progressive degradation that leads to complete breakdown.

At 1 kc the maximum attainable voltage caused breakdown in about 60 seconds at a stress of 4.5 KV/mil. Therefore, higher voltages would be required in order to reduce the duration of the test. The same situation prevails at 38 kc, as shown by the data in Table VII.

A complete discussion of these results would be premature. Additional data, particularly on other materials, are required before a detailed analysis is warranted. A considerable amount of data on the effect of frequency on electric strength have been accumulated in the course of several investigations. In these previous studies, however, primary consideration was given to the effects of temperature and moisture absorption. Consequently, large numbers of specimens were involved and attention was focused on the detection of relatively large changes in properties. The present study was more concerned with determining the mechanisms that lead to breakdown over the frequency range from 60 cps to 18 mc so that the high-frequency behavior could be more accurately predicted in practical situations. Therefore, it was possible to employ a more elaborate specimen which permitted a thinner section to be tested. This resulted in higher values of electric strength than those obtained on polystyrene in previous programs.

Electric strength measurements on other materials were not made, however, because priority was given to the calorimetric measurement of dielectric losses at high electrical stresses in the r-f range.

D. Calorimetric Measurement of Dielectric Losses at High Electrical Stresses in the Radio Frequency Range.

1. General Remarks

When an alternating electric stress is applied to a dielectric a certain amount of power will be dissipated in the dielectric material. In a vacuum environment where the removal of heat from a component can be a difficult design problem, the heat generated in dielectric parts must be given careful consideration, particularly in r-f applications. At very low stresses, the power dissipation per unit volume (W/cm^3) can be computed from the values of loss factor (ϵ' tanδ) that are measured with low-voltage devices. At higher stresses, the computed values of W/cm^3 can be in error if loss factor is stress dependent.

In the course of previous studies at this laboratory, it was found that the computed values of W/cm^3 at breakdown, when plotted as a function of frequency, did not agree with qualitative observations made during breakdown (electric strength) measurements in the r-f range. Corrections for the temperature dependence of loss factor did not account for the discrepancies, so the apparent higher losses at high stresses must have been caused by an increase in loss factor with increasing stress or the generation of heat by a process that was not associated with dielectric loss in the specimen, such as electrical discharges.

The purpose of the present investigation is two-fold: (a) to determine the relationship between loss factor and field strength at frequencies in the r-f range; and (b) to relate these results to the breakdown of dielectrics in the r-f range.

Loss measurements can be made at high stresses with various types of high-voltage bridges that operate at low frequencies. At high frequencies, however, such measurements can not readily be made at high voltages. It is possible, however, to directly measure the power dissipated in a dielectric specimen at high stresses using a calorimetric method. Such measurements permit the stress dependence of loss factor to be investigated and the values of W/cm^3 to be related to tanδ.

D. Calorimetric Measurement of Dielectric Losses at High Electrical Stresses in the Radio Frequency Range.

1. General Remarks

When an alternating electric stress is applied to a dielectric a certain amount of power will be dissipated in the dielectric material. In a vacuum environment where the removal of heat from a component can be a difficult design problem, the heat generated in dielectric parts must be given careful consideration, particularly in r-f applications. At very low stresses, the power dissipation per unit volume (W/cm^3) can be computed from the values of loss factor (ϵ' tanδ) that are measured with low-voltage devices. At higher stresses, the computed values of W/cm^3 can be in error if loss factor is stress dependent.

In the course of previous studies at this laboratory, it was found that the computed values of W/cm^3 at breakdown, when plotted as a function of frequency, did not agree with qualitative observations made during breakdown (electric strength) measurements in the r-f range. Corrections for the temperature dependence of loss factor did not account for the discrepancies, so the apparent higher losses at high stresses must have been caused by an increase in loss factor with increasing stress or the generation of heat by a process that was not associated with dielectric loss in the specimen, such as electrical discharges.

The purpose of the present investigation is two-fold: (a) to determine the relationship between loss factor and field strength at frequencies in the r-f range; and (b) to relate these results to the breakdown of dielectrics in the r-f range.

Loss measurements can be made at high stresses with various types of high-voltage bridges that operate at low frequencies. At high frequencies, however, such measurements can not readily be made at high voltages. It is possible, however, to directly measure the power dissipated in a dielectric specimen at high stresses using a calorimetric method. Such measurements permit the stress dependence of loss factor tδ be investigated and the values of W/cm^3 to be related to tanδ.

At a given frequency a dielectric specimen can be represented as a pure capacitance, C, in parallel with a resistance, R, as shown in Figure 18. The dissipation factor of such a specimen is given by the ratio W_d/VI_C, where W_d is the power dissipation in the specimen, V is the applied voltage and I_C is the capacitive current. W_d can be measured with the calorimeter, V can be measured directly and I_C can be computed from the measured values of V and the specimen capacitance, C. It will be shown later that these values do not have to be known if it is only desired to determine if loss factor varies with the square of the applied voltage.

It should be noted that if R or C is voltage dependent, the current and voltage will contain harmonic components. Under such conditions it is desirable to minimize the harmonic components of the voltage.

A calorimeter has been designed and built and loss measurements have been made. The theory of operation and design details are discussed in the following sections.

Other workers have used thermal measurements to determine the losses in dielectrics. Race and Leonard[6] describe two methods that were used successfully, but neither of these methods was applicable to the present investigation where the measurements were made at relatively high stresses.

2. Theory of Operation

In the most common type of calorimeter, the total energy transferred from the specimen to a body of known heat capacitance is determined by measuring the temperature rise of the body. The total energy Q is given by:

$$Q = \int_0^t W_d dt = h \int_{t=0}^{t=t} dT,$$

where W_d is the power dissipation in the specimen, h is the heat capacitance, t is time and T is the temperature of the body. If W_d does not vary with

time, it can be determined by measuring Q for a known time interval. The advantage of this method is that W_d can be determined accurately by waiting until the temperature rise is large enough to be easily measured. However, it is necessary to insulate the device so that the heat leak is negligible. This requirement is difficult to meet when the specimen is a slab of dielectric that must be placed between metal electrodes and connected to an r-f tank circuit. The electrical leads must be relatively large because of the high currents that are encountered at high stresses and, therefore, the heat leak through the leads cannot be neglected. The current is about 4 amps at 2 mc for a 4 mil polystyrene specimen at a stress of 2000 VPM.

An alternative method consists of measuring the heat flow from the dielectric specimen to a heat sink of known temperature through a conductor of known thermal properties. The conductor must have a thermal conductance that is high enough so that practically all of the heat developed in the specimen will flow through the conductor to the heat sink. The power dissipated in the specimen is determined by measuring the temperature difference between the heat sink and a point on the conductor.

Figure 19 illustrates the operating principle of the calorimeter. Two identical conductors of constant cross-sectional area, A, serve as electrical leads to the r-f generator and as thermal conductors between the specimen and the heat sinks. The specimen is located at x=0 and the heat sinks are located at x=L and x=-L respectively. The specimen thickness is small compared to L, so the heat source can be considered to be concentrated at x=0.

Heating of the leads by the r-f current is a source of error which modifies the well known equations for heat flow along a conducting bar. It can be shown that in the steady state, i.e., when T_x has reached an equilibrium value, the heat flow in the x-direction is given by

$$1/2\, W_d + \int_0^x w_r dx = -KA \frac{dT}{dx}$$

where w_r is the power dissipation per unit length caused by r-f heating and

K is the coefficient of thermal conduction of the lead. This follows from the symmetry of the thermal circuit and the fact that all heat developed by the specimen at x=0 and all heat developed by r-f heating flows away from x=0.

Since w_r is independent of x, the total power developed by r-f heating between x=0 and any point x is $w_r x$. Therefore, the power dissipation in the specimen is

$$W_d = -2\left(KA\frac{dT}{dx} + w_r x\right)$$

The solution for the temperature T_x at any point x is

$$T_x = \frac{1}{2KA}\left\{W_d(L-x) + w_r(L^2 - x^2)\right\} + T_L$$

The temperature difference, θ_x, between x=0 and any point x is

$$\theta_x = \frac{1}{2KA}\left(W_d x + w_r x^2\right)$$

Figure 20 shows the temperature distribution along the heat leads which results from the linear contribution from the power dissipated in the specimen and the quadratic contribution from the r-f heating in the leads. To keep the error caused by r-f heating small, the ratio $w_r x/W_d$ should be small. This indicates that the r-f resistance of the leads should be as low as possible and the temperature difference should be measured between x=0 and a point close to x=0, so that x will be small. It is convenient, however, to measure the temperature difference, θ_L, between x=0 and the heat sink at x=L. Therefore, L should be kept small. But, for a given power dissipation in the specimen, θ_L decreases as L is decreased and this reduces the sensitivity. Therefore, it is necessary to effect a design compromise between the desired sensitivity and the allowable error introduced by r-f heating.

Any heat that is developed in the dielectric specimen and does not flow through the heat conductors to the heat sinks constitutes a heat leak, causing an error in the measurements. To keep the heat leak small, the conductance of the leads should be high compared to the conductance of the medium that surrounds the leads and the specimen. A further reduction can

be achieved by surrounding the immersion medium with walls that are maintained at a temperature close to the temperature of the leads and the specimen. This temperature will, of course, be the same as the heat sink temperature.

An inexpensive calorimeter based on the operating principles discussed above is described in the following section.

3. Design of Calorimeter

Because it was intended to make measurements at high-voltage in the r-f range, the electrical requirements were severe. To eliminate corona it was necessary to surround the specimen and the electrodes with a high-strength medium. From the thermal considerations it would have been desirable to use a vacuum or a compressed gas as the immersion medium. However, the complications introduced by requiring a pressure-tight vessel made these choices unattractive for a preliminary model. Transformer oil was selected as the immersion medium because it permitted the design to be greatly simplified and, as shown below, it has acceptable thermal properties.

The other severe electrical requirement was associated with the high r-f currents that are encountered with specimens of reasonable size. For example, at 2 mc a polystyrene sample of 3.5 mil thickness and an area of 2.3 cm^2 has a capacitance of about 57 pf and at 7 KV the specimen current is 5 amps. The resistance of a 3/4 inch diameter brass conductor at 2 mc is about 0.0006 ohms/inch. Therefore, the power dissipation per inch is about 0.6 milliwatts/amp. At higher frequencies the error introduced by r-f heating at a given voltage is greater because the skin resistance increases with the square root of frequency and the current increases linearly with frequency, so the losses increase in proportion to the 3/2 power of frequency. The dielectric loss in the specimen, however, is proportional to frequency if the loss factor does not change significantly. Therefore, the error introduced by resistive heating of the leads becomes greater as the frequency is increased.

To meet these electrical requirements and the thermal requirements discussed in the previous section, the essential parts of the calorimeter

were arranged as shown in Figure 21. The leads to the specimen serve as heat conductors and electrical connections. They are made of 3/4 inch diameter brass tubing with 1/32 inch wall thickness and are 1 1/2 inches long. One end of each tube is closed off with a flat copper plate that makes electrical and thermal contact to the specimen. The other end of each tube is bonded to a copper heat sink. The lower heat sink is part of the metal vessel that contains the immersion medium. The space between this vessel and the outer container is packed with melting ice. The upper heat sink consists of a smaller metal vessel that is connected to the r-f lead. The smaller ice-filled container is at high potential during the experiment. Both the upper and lower heat sinks have cooling fins to provide a more stable temperature at the base of each heat lead.

Brass was used for the leads merely for the sake of convenience. These leads could be silver plated or replaced by copper leads if the experiments indicated that further refinements are justified. The leads were also made so that they could be readily replaced with other leads of different conductance. This would extend the useful range of the calorimeter.

A heat sink temperature of $0^{\circ}C$ was also chosen for convenience. A more elaborate calorimeter could be built for experiments at elevated temperatures.

To minimize the heat leak through the oil, the larger metal container is 6 inches in diameter, which is eight times the diameter of the heat leads. The upper container has a diameter of 3 inches, so that a spacing of 1 1/2 inches is provided to withstand the high voltage between the inner and outer containers.

The detailed construction of the lower (ground) lead is shown in Figure 22. A thermistor is imbedded in the plate that makes contact with the dielectric sample. A Wheatstone bridge is used to measure the resistance of the thermistor. Because the upper lead is at high-voltage, it would be difficult to measure the heat flow to the upper heat sink. To eliminate this requirement, the specimen and the heat leads are made symmetrical so that the heat flow in each lead is the same. Therefore, the total power dissipated in the specimen is twice the value determined by the heat flow in the lower lead.

The heat loss through the oil, W_0, can be estimated by the relationship

$$W_0 = \Delta T \frac{2\pi K_0 L}{\ln(a/b)}$$

where ΔT is the average temperature difference between the leads and the container, K_0 is the thermal conductivity of the oil, a is the radius of the container and b is the radius of the leads. For $\Delta T=1^{\circ}C$, a/b=8, L=8cm, and $K_0=0.16$, the heat flow through the oil is 38 milliwatts. This much heat loss would occur when the power dissipation in the specimen is about 1 watt, so the heat leak is small compared to the measured wattage. The error is actually eliminated by the calibration procedure, but it can be seen that the heat leak through the oil is small enough so that minor variations caused by movement of the oil or changes in properties from one batch of oil to another would not affect the calibration.

Although the thermal and electrical analyses provide the information required to design the calorimeter, the actual calibration is based on the dissipation of a known wattage in a dummy specimen.

4. Calibration

As shown in Figure 22, a thermistor is embedded in the face of the lower heat lead, and the resistance of the thermistor is measured with a Wheatstone bridge. The resistance of a thermistor varies with temperature according to the relationship.

$$R_1/R_0 = e^{-\gamma(T_1 - T_0)}$$

where R_1 and R_0 are the resistances at temperatures T_1 and T_0 respectively, and γ is a constant for a particular thermistor. If T_0 is the heat sink temperature ($0^{\circ}C$) and T_1 is the equilibrium temperature of the thermistor when the power dissipation in the specimen is W_d, then according to the law of heat conduction

$$T_1 - T_0 = W_d c$$

where c is a constant of the heat leads. Therefore, it follows that

$$R_1/R_0 = e^{-\gamma c W_d}$$

To calibrate the calorimeter in terms of R_1/R_0 and W_d, a known heat flow is introduced into the leads by a heating element. This heating element is built into a dummy specimen so that the heat transfer characteristics are essentially the same as those of a dielectric specimen. The heater is energized with a battery and the input power is controlled with a series resistor. Measurements of R_1 and R_0 are made after transient effects have disappeared. For small enough values of W_d the plot of W_d vs. R_1 lies on a straight line, as shown in Figure 23. Of course, the calibration curve applies only to a fixed set of conditions, so a modification in the heat leads would necessitate recalibration. Adjustments can also be made in the specimen thickness to vary the total wattage for a given stress. If the thickness is reduced, the smaller volume will develop less total heat for a given stress. On the other hand, increasing the thickness would result in an increased wattage for a given stress.

The measurement of power dissipated in the specimen is made without actually determining the temperature of the specimen. However, for the purposes of estimating experimental errors it is convenient to know the approximate temperature rise for a given wattage. This temperature can be approximated by calculating the thermistor temperature from the relationships previously mentioned. The specimen temperature is nearly equal to the thermistor temperature and it varies with W_d in a linear manner, as shown in Figure 24.

5. Limitations Imposed by the Use of Continuous Voltages

When dielectric losses are measured as a function of field strength with this type of calorimeter, the voltage is increased in steps and sufficient time must be allowed at each step for the temperature of the specimen to stabilize. It was found that periods of 10 to 30 minutes were required, depending on the magnitude of the incremental increase in applied voltage. This relatively long-time application of voltage imposes a limitation on the maximum stress that can be used without causing the specimen to fail. With polystyrene, for example, measurements on 10 mil specimens could not be made at stresses exceeding 400 VPM.

A second limitation is encountered when measurements are to be made over a wide range of stresses. If, for example, it is desirable to

make measurements from 30 to 1800 VPM, a ratio of 1:60, the power dissipated in the specimen would have a range of 1:3600. To cover such a range, major adjustments would have to be made in the conductance of the heat leads to prevent intolerable heating of the specimen. Therefore, it would be necessary to interrupt an experiment to replace heat leads whenever the temperature of the specimen reached a predetermined limit. The experiment itself would become more difficult because uniform thermal contact between the heat lead and the specimen becomes more important as the conductance of the heat lead is increased.

Another source of difficulty at high stresses is associated with the design of a suitable heat sink. The power dissipation in a typical 10 mil polystyrene specimen at 2 mc is about 0.2 watts for an applied stress of 100 VPM, but at 1800 VPM it would be 65 watts. A suitable heat sink would have to absorb this power without allowing a temperature rise of more than $0.1^{\circ}C$ at the end of the heat lead that is bonded to the heat sink.

These difficulties, which are encountered when continuous r-f voltages are used, can be avoided by drastically reducing the time of voltage application. The benefits of using short pulses, rather than continuous voltages, are twofold: (a) the specimen can withstand a higher voltage, and (b) excessive power dissipation in the specimen is avoided.

Consideration was given to a single-pulse technique, but the difficulties associated with the transient heat measurement makes this method unattractive for the purposes of the present investigation. Instead, a method was developed in which repeated r-f pulses were applied to the specimen. The repetition rate and pulse width are not critical as long as the temperature fluctuations remain negligible. The maximum stress at which measurements can be made is lower than it would be for the single-pulse method, but it is considerably higher (up to 2050 VPM for polystyrene) than for the continuous voltage method that was used in the earlier experiments.

6. Repeated Pulse Method

Using the repeated-pulse method, an initial measurement of power dissipated per unit volume (Watts/cm^3) is made by applying a continuous r-f field at some low stress E_1. The technique used in this first step and

the method of calculating tanδ from the experimental data are discussed in Section 1. The stress is then increased to a value E_2, but it is now applied in repeated pulses, with a repetition rate and pulse width that result in the same average power dissipation as the continuously applied stress E_1. The average power dissipation, W, depends on the ratio α/β, where α is the pulse duration and β is the time from the beginning of one pulse to the beginning of the next pulse, i.e., the reciprocal of the repetition rate.

The stress is then increased to successively higher levels and at each step the ratio α/β is adjusted so that the average power dissipation remains the same. This can be accomplished by changing α, β or both α and β.

The instantaneous power dissipation, W', is given by

$$W' = (\beta/\alpha)\, W$$

It is W' that is a measure of the loss factor, ϵ'', and if ϵ'' is independent of the applied stress, E, then W' should be proportional to E^2.

To determine if ϵ'' is a function of E, it is only necessary to measure the values of E, α and β that result in a constant value W at each step in the stress range of interest. At any two stress levels, E_n, E_m, the following relations hold:

$$W'_m = (\beta_m/\alpha_m)\,(\alpha_n/\beta_n)\, W'_n \qquad (1)$$

and

$$W'_m/W'_n = (E_m/E_n)^2, \text{ for constant } \epsilon''. \qquad (2)$$

Since

$$(E_m/E_n)^2\,(W'_n/W'_m) = 1,$$

then, substituting from equation (1),

$$(E_m/E_n)^2\,(\beta_n/\alpha_n)\,(\alpha_m/\beta_m) = 1. \qquad (3)$$

If ϵ'' is a function of E, then the measured values of E, α and β do not yield a value of unity in equation (3).

In the former method, where continuous stresses were applied, a considerable length of time was required at each stress level for the temperature of the specimen to stabilize. In the present method, this will occur only for the first step, where the stress is low. From there on, with some experience in adjusting α and β, the temperature fluctuations

can be kept small and the time required for temperature stabilization is drastically reduced.

Because the specimen temperature is adjusted to the same value throughout the experiment, the calorimeter serves only as a sensitive temperature difference indicator. The average thermodynamic conditions remain the same at each stress level, so the inherent errors in the calorimeter have no significant effect on the ratios of the measured loss factors. The largest error is made in the measurement of the actual value of ϵ'' in the first step of the experiment. This error could be reduced by constructing a calorimeter that is designed specifically for measurements at low stresses.

7. The Dielectric Specimen

The specimen was previously referred to as a dielectric "slab", but this is an oversimplification. If the calorimeter is to be used at high stresses, the specimen/electrode arrangement is the most critical part of the device.

To avoid breakdown at relatively low stresses, it is necessary to use recessed electrodes and to provide intimate electrical contact with the specimen by applying a conductive coating to the cavities. Such specimens have been developed for use in electric strength measurements in the r-f range. They have been used successfully at stresses up to 2600 VPM at 2 mc. This particular type of specimen, however, does not have a uniform thickness at the base of the cavity. The high-voltage electrode fits into a circular groove and the thinnest portion of the specimen is located between the bottom of the groove and the flat face of the sample that is in contact with the ground electrode. This configuration is not well suited for loss measurements with the calorimeter because the field is not uniform in the entire volume that contributes to the generated heat. It would, therefore, be difficult to reduce the measured values of watts to values of watts per unit volume.

The ideal specimen for use in the calorimeter would be one that has a uniform thickness over the area between the electrodes. Since it is necessary to use recessed electrodes to avoid discharges, a flat bottomed cavity could be used. The power dissipated per unit volume, W_d, would be

negligible in the thick portion of the specimen because W_d varies with the square of the field strength. An abrupt change in thickness, however, results in a sharp corner at the periphery of the cavity, causing stress concentration that leads to breakdowns at relatively low voltages. It is necessary, therefore, to compromise and round off the edges of the cavity, as shown in Figure 25.

The error introduced by the nonuniform field around the edge of the cavity can be kept small by making the diameter of the cavity large. The heat produced at the edge is proportional to the diameter, while the heat produced over the flat portion is proportional to the square of the diameter. The area at the base of the cavity cannot be made too large, however, because of difficulty in machining a thin section of large area. As shown in Figure 25, a 3/4 inch diameter cavity with a 1/16 inch edge radius was used.

The specimen is made from two blocks of material, 1/2" x 1 3/4" x 1 3/4". The upper part of the specimen contains the flat-bottomed cavity, the lower part has a 3/4 inch hole drilled through its entire thickness. The bottom of the cavity and a circular area on the bottom face of the thin section is coated with evaporated silver. To provide symmetrical heat flow, the two parts are cemented together, as shown in Figure 25. The space between the blocks is exaggerated in the drawing, they actually make intimate contact.

Any heat produced outside the test volume increases the error of the loss measurements. The r-f heating of the heat leads, for example, has already been discussed. The r-f current can also cause heating at the area of contact between the specimen and the end plate of the heat lead. To provide better contact, both faces of the critical volume were silver coated, as shown in Figure 25. In addition, a disc of 1-mil aluminum foil was inserted between the specimens and the end plate of each heat lead. The aluminum foil not only provides improved contact, but it also protects the specimen from mechanical damage.

Another source of undesired heat is the presence of discharges or corona on the heat leads or electrodes. This problem was encountered in a series of measurements on 10-mil polystyrene samples. An apparent increase in loss factor was observed on those specimens that showed evidence

of tracking. One method of eliminating the difficulty is to reduce the thickness of the specimen so that the measurements can be made at a lower voltage. Other factors must be considered, however, in reducing the thickness of the specimen: (a) it becomes increasingly difficult to fabricate the specimen as the thickness is reduced; (b) for a given stress, the wattage in the specimen is proportional to thickness, d, and (c) for a given voltage, the heat generated by the r-f current is proportional $1/d^2$. Therefore, the specimen must be thin enough so that discharges do not occur, but thick enough so that the r-f heating is not too great and the dissipated wattage is large enough to be measured.

8. Experimental

The final model of the calorimeter was designed and constructed in the latter part of the program. Most of the effort that could be effectively applied to this phase of the program was devoted to the development of the overall technique. A considerable effort was involved in achieving suitable repeated pulses for the measurements at 2 mc.

Many specimens were tested in the course of the investigation, but most of the results were useful only in providing information that could be used in improving the method. The procedure was never routine. Many specimens were tested before a valid measurement was obtained. Consequently, time did not permit the accumulation of a large amount of data.

Successful measurements were made at 2 mc on polystyrene (Styron 666 samples) as follows:

(a) Thickness = 3.4 mils.
Continuous voltage applied = 1.05 KV.
Stress at 1.05 KV , 308 VPM.
Highest pulse voltage = 7.0 KV.
Stress at 7.0 KV = 2050 VPM, pulse length = 7 milliseconds, repetition time 261 milliseconds.
Specimen temperature = 6.0°C.
Average dissipated power = 0.7 watts.
tanδ at 308 VPM = 0.00086.
Ratio of loss factor at 2050 VPM to that at 308 VPM = 0.84.

(b) Thickness = 6 mils.
Continuous voltage applied = 1.09 KV.
Stress at 1.09 KV = 182 VPM.
Pulsed voltage applied = 1.74 KV.
Stress at 1.74 KV = 259 VPM, pulse length 8.9 milliseconds, pulse repetition time = 21.9 milliseconds.
Specimen temperature = 4.2°C.
Average dissipated power = 0.45 watts.
Tanδ at 182 VPM = 0.00095.
Ratio of loss factor at 259 VPM to that at 182 VPM = 0.98.

In both cases the apparent loss factor decreased with increasing stress. Furthermore, comparing the values of tanδ for the continuous voltages used in (a) and (b), the higher stress (308 VPM)yielded a lower value. These measurements indicate that the power dissipated per unit volume is less than proportional to the square of the applied stress. Further analysis, particularly with regard to harmonic content of the applied voltage would be required to determine if the measured differences are significant.

The important conclusion, however, is that loss factor does not increase with applied stress. Therefore, low-voltage loss measurements provide conservative design data for use at higher stresses.

The results, of course, pertain to polystyrene at 2 mc. Time did not permit further extension of the study to include other materials or other frequencies.

E. High Temperature Loss Measurements

In addition to measuring dielectric losses at high field strengths in the r-f range, loss measurements were made at high temperatures so that the data would be available for correlation purposes. To facilitate loss measurements at frequencies up to 30 mc and temperatures up to 300°C, a special two-electrode cell was designed and constructed. This stainless steel cell consisted of a 1 1/2" diameter thin-walled cylinder, 3 3/4" long, closed at one end with a 3/4" thick plug. The plug served as the grounded electrode. Heating wires were wrapped on the outside of this cylinder. The ungrounded electrode (1" diameter x 1/8" thick) was supported by a 1/8" diameter thin-walled tube, 3 1/2" long. This tube, which provided the means of electrical contact with the measurement circuit, constituted

the major heat leak. Therefore, it was surrounded by a separate heater consisting of a 1" diameter cylinder with heater wires wrapped on the outside. The ungrounded electrode and its lead were supported by a Teflon bushing on the outside and a quartz collar on the inside. A 3" diameter cylinder served as an outer heat shield for the entire cell. Temperature was measured with a thermocouple mounted in a well in the ground electrode. Those parts that introduce series resistance were heavily silver-plated to reduce the high frequency resistance to a minimum.

The cell was designed for use with a Q-meter (Boonton Model 260A) at frequencies of 2 to 30 mc. Calibration checks were made at lower frequencies (100 cps to 100 kc) using a Shering bridge.

The specimens consisted of 1 3/8" diameter discs, 12 to 15 mils thick, with evaporated silver electrodes. The ungrounded electrode had a 1" diameter and the grounded electrode had a 1 1/4" diameter.

Several experimental runs were made using a temperature rise of about 0.7°C per minute. Measurements were made at 5°C intervals up to 200°C or to the softening point of the specimen.

Measurements of this type yield data in the form of capacitance and dissipation factor values. The capacitance data can be reduced to values of dielectric constant by applying an appropriate cell factor. The cell factor, however, depends on the dimensions of the specimen (area to thickness ratio) so it would depend on temperature. With polymeric materials that have coefficients of expansion in the order of 5×10^{-5} per °C at room temperature, significant corrections would be required in applying the cell factors. Such corrections could not be made to the data obtained in this phase of the program because the information on the coefficients of expansion over the applicable temperature range was not readily available. This supplementary data would have been obtained if the program had been continued and the results of the calorimetric measurements of tanδ had warranted the additional refinement.

The results that were obtained in this study are summarized below. The capacitance data are presented in terms of the percentage decrease from

room-temperature values. Measurements were made on TFE, FEP, Styron 666 (polystyrene), C-1147 (methyl styrene with dimethyl siloxane additive) and Alathon-10 (polyethylene).

1. TFE-7

TFE-7 exhibited smaller changes than the other materials. The capacitance decreased slowly with increasing temperature. The 200°C values were about 6% less than the room-temperature value over the frequency range from 100 cps to 30 mc. Therefore, the temperature coefficient of capacitance was about .034% per °C. Dissipation factor also decreased with increasing temperature at the lower frequencies. At 100 cps, tanδ decreased from 0.0005 at 25°C to 0.0002 at 200°C. At 100 kc the corresponding values were 0.0003 at 25°C and 0.0001 at 200°C. At the higher frequencies (1 to 30 mc) the values were about 0.0001 over the entire temperature range.

2. FEP-100

Somewhat larger changes were observed with FEP-100, as shown by the data of Tables VIII and IX. Again, both capacitance and tanδ decreased with increasing temperature.

3. Alathon-10

Because of its low softening temperature (94°C) measurements could not be made on Alathon-10 at temperatures above 115°C. Up to 60°C, capacitance decreased by only 3% and up to 90°C it decreased by about 8%. Rapid changes then occurred as the material softened and the separation between the electrodes decreased.

Only slight changes in dissipation factor were observed up to 115°C , which is above the melting point. Below 100 kc, tanδ decreased from 0.0003 at 25°C to 0.0002 at 115°C. At the higher frequencies, the corresponding change was from 0.0002 to 0.0001.

4. C-1147

C-1147, which is a methyl styrene with a dimethyl siloxane additive, exhibited slight changes in capacitance (1.5 to 2.0%) up to 100°C. At 140°C the decrease was 3.5% at 100 cps and 5.7% at 30 mc.

The tanδ data are shown in Figure 26. The peaks in the tanδ vs. temperature curves are typical of a dipolar material.

5. Styron 666

This polystyrene material exhibited a slowly decreasing capacitance up to 70°C (about 1%), but then showed a more rapid change, reaching about 5% at 150°C with only slight differences over the entire frequency range.

The tanδ data are summarized in Figure 27. The behavior is similar to that exhibited by C-1147, except that the peak value for a particular frequency occurs at a lower temperature and all of the values are lower than those for C-1147. This data would indicate that there was a dipolar impurity in this particular group of specimens.

As mentioned previously, this study was planned as a supplement to the investigation of the high field strength phenomena. The purpose was to develop the means of providing data on the high temperature loss characteristics of materials that were to be used in the high field strength investigations. The data that were obtained during this development has been included herein because it is of general interest. However, no attempt was made to conduct a systematic study of temperature effects that could be used in determining the structural dependence of dielectric properties.

IV. Anticipated Work

The activities of the Dielectrics Laboratory will be discontinued on June 30, 1964. Therefore, this work will not be continued at the Johns Hopkins University.

V. Level of Effort

The total level of effort during the 15-month period from April 1, 1963 to June 30, 1964 was approximately 92 man-months.

VI. Professional Staff

Louis J. Frisco	Research Contract Director, M.Sc. in Electrical Engineering. Full time.
A.M. Muhlbaum	Research Associate, Dipl. in Engineering Physics (Technical University of Delft, Netherlands). Full time.
E.A. Szymkowiak	Research Staff Assistant, B.E. in Electrical Engineering. Full time.

VII. References

1. Final Report of Contract DA-36-039-SC-89147, March 1, 1962 to March 31, 1963, "Dielectrics for Satellites and Space Vehicles". The Johns Hopkins University, Dielectrics Laboratory. Available through ASTIA.
2. J.F. Fowler, "X-Ray Induced Conductivity in Insulating Materials". Proceedings of the Royal Society, Vol. 236A, p. 464-80 (1956).
3. L.E. Amborski, "Structural Dependence of the Electrical Conductivity of Polyethylene Terephthalate". J. Polymer Sci., Vol. 62, p. 331-46 (1962).
4. L.A. Wall and R.E. Florin, "Polytetrafluoroethylene - A Radiation Resistant Polymer." Letter to the Editor, J. Appl. Polymer Sci., Vol. II, No. 5, p. 251 (1959).
5. C.G. Garton, "Dielectric Loss in Thin Films of Insulating Liquids". J. Inst. Elect. Eng., 88, II, 103-120 (1941).
6. H.H. Race and S.C. Leonard, "Calorimetric Measurements of Dielectric Losses in Solids". Electrical Engineering, Vol. 55, No. 12, p. 1347-56 (1936).

Table I. TFE-7 Vacuum X-Ray Exposure and Recovery Data at 28°C; Dose Rate 0.2 Mrads Per Hour.

Absorbed Dose (Mrads)	Dielectric Constant				Dissipation Factor			
	100 cps	1 kc	10kc	100 kc	100 cps	1 kc	10 kc	100 kc
0	2.109	2.107	2.107	2.107	.0002	.0002	.0002	.0002
.10	2.109	2.107	2.107	2.107	.0005	.0003	.0001	.0001
.20	2.109	2.107	2.107	2.107	.0006	.0003	.0001	.0001
.30	2.109	2.109	2.109	2.109	.0006	.0003	.0001	.0001
.41	2.113	2.111	2.111	2.111	.0006	.0003	.0001	.0001
.51	2.113	2.111	2.111	2.111	.0006	.0003	.0001	.0001
.61	2.115	2.111	2.111	2.111	.0008	.0002	.0001	.0001
.71	2.115	2.113	2.111	2.111	.0009	.0003	.0001	.0001
.81	2.115	2.115	2.111	2.111	.0010	.0004	.0002	.0002
.91	2.115	2.115	2.113	2.113	.0018	.0004	.0002	.0002
.96	2.117	2.115	2.113	2.113	.0026	.0006	.0002	.0002
1.01	2.117	2.115	2.113	2.113	.0048	.0008	.0002	.0002
1.06	2.119	2.115	2.113	2.113	.0072	.0012	.0003	.0002
1.11	2.123	2.115	2.113	2.113	.0136	.0022	.0003	.0002
1.16	2.127	2.115	2.113	2.113	.0211	.0033	.0005	.0002
1.21	2.133	2.117	2.113	2.113	.0263	.0045	.0007	.0002
1.27	2.142	2.117	2.113	2.113	.0378	.0057	.0008	.0003
1.32	2.150	2.119	2.115	2.115	.0472	.0069	.0010	.0003
1.37	2.156	2.119	2.115	2.115	.0568	.0083	.0012	.0004
1.42	2.164	2.119	2.115	2.115	.0644	.0097	.0014	.0004
1.47	2.168	2.121	2.115	2.115	.0758	.0112	.0015	.0005
1.52	2.174	2.121	2.115	2.115	.0844	.0120	.0017	.0005
1.57	2.180	2.121	2.115	2.115	.0911	.0129	.0018	.0005
1.62	2.195	2.121	2.115	2.115	.0985	.0139	.0019	.0005
1.67	2.187	2.121	2.115	2.115	.104	.0146	.0020	.0005
1.72	2.189	2.123	2.115	2.115	.110	.0152	.0021	.0005
1.77	2.191	2.123	2.115	2.115	.113	.0157	.0021	.0005
1.82	2.191	2.123	2.115	2.115	.116	.0160	.0021	.0005
4.85	2.131	2.123	2.121	2.121	.0166	.0025	.0005	.0003
6.27	2.125	2.123	2.123	2.123	.0044	.0008	.0002	.0002
10.9	2.127	2.123	2.123	2.123	.0008	.0004	.0002	.0002
Recovery Data (Hours)								
1	2.127	2.125	2.123	2.123	.0016	.0006	.0004	.0003
3	2.127	2.125	2.123	2.123	.0030	.0006	.0004	.0003
7	2.129	2.129	2.125	2.125	.0040	.0008	.0004	.0003
24	2.131	2.129	2.127	2.127	.0016	.0009	.0003	.0002
120	2.131	2.129	2.127	2.127	.0015	.0008	.0002	.0002

Table II. FEP-100 Vacuum X-Ray Exposure Data; Dose Rate 0.2 Mrads Per Hour.

Absorbed Dose (Mrads)	Dielectric Constant				Dissipation Factor			
	100 cps	1 kc	10 kc	100 kc	100 cps	1 kc	10 kc	100 kc
0	2.133	2.133	2.133	2.133	.0003	.0002	.0002	.0002
.10	2.133	2.133	2.133	2.133	.0003	.0002	.0002	.0002
.15	2.133	2.133	2.133	2.133	.0003	.0002	.0002	.0002
.20	2.133	2.133	2.133	2.133	.0003	.0002	.0002	.0002
.30	2.133	2.133	2.133	2.133	.0004	.0002	.0002	.0002
.40	2.133	2.133	2.133	2.133	.0004	.0002	.0002	.0002
.51	2.133	2.133	2.133	2.133	.0004	.0002	.0002	.0002
.61	2.133	2.133	2.133	2.133	.0004	.0002	.0002	.0002
.71	2.133	2.133	2.133	2.133	.0003	.0002	.0002	.0002
.81	2.133	2.133	2.133	2.133	.0003	.0002	.0002	.0002
1.01	2.133	2.133	2.133	2.133	.0003	.0002	.0002	.0002
1.22	2.133	2.133	2.133	2.133	.0004	.0002	.0002	.0002
1.42	2.133	2.133	2.133	2.133	.0004	.0003	.0002	.0002
1.82	2.131	2.131	2.131	2.131	.0005	.0004	.0002	.0002
2.03	2.129	2.129	2.129	2.129	.0012	.0004	.0002	.0002
2.13	2.129	2.129	2.129	2.127	.0015	.0004	.0002	.0002
2.23	2.129	2.129	2.129	2.127	.0018	.0004	.0002	.0002
2.33	2.129	2.129	2.129	2.127	.0022	.0004	.0002	.0002
2.43	2.129	2.129	2.127	2.127	.0023	.0004	.0002	.0002
2.53	2.129	2.129	2.127	2.127	.0027	.0005	.0002	.0002
2.63	2.129	2.129	2.127	2.127	.0031	.0005	.0002	.0002
2.73	2.129	2.129	2.127	2.127	.0033	.0005	.0002	.0002
2.83	3.129	2.127	2.127	2.127	.0037	.0005	.0002	.0002
2.93	2.129	2.127	2.127	2.127	.0039	.0005	.0002	.0002
3.04	2.129	2.127	2.127	2.127	.0040	.0006	.0002	.0002
3.24	2.129	2.127	2.127	2.127	.0043	.0007	.0002	.0002
3.34	2.129	2.127	2.127	2.125	.0046	.0007	.0002	.0002
3.44	2.129	2.127	2.125	2.125	.0047	.0007	.0002	.0002
3.54	2.129	2.127	2.125	2.125	.0051	.0007	.0002	.0002
3.64	2.129	2.127	2.125	2.125	.0052	.0007	.0002	.0002
3.74	2.128	2.127	2.125	2.125	.0052	.0008	.0002	.0002
3.85	2.128	2.127	2.125	2.125	.0053	.0008	.0002	.0002
3.95	2.128	2.127	2.125	2.125	.0053	.0008	.0002	.0002
4.04	2.128	2.127	2.125	2.125	.0054	.0008	.0002	.0002
4.75	2.128	2.127	2.125	2.125	.0054	.0008	.0002	.0002
4.86	2.128	2.127	2.125	2.125	.0054	.0008	.0002	.0002
4.95	2.126	2.126	2.125	2.125	.0054	.0008	.0002	.0002
5.26	2.126	2.126	2.125	2.125	.0053	.0009	.0002	.0002
6.07	2.126	2.126	2.125	2.125	.0050	.0009	.0002	.0002
6.47	2.126	2.126	2.125	2.125	.0048	.0009	.0002	.0002

Table II. (continued)

FEP-100 Vacuum X-Ray Exposure Data; Dose Rate 0.2 Mrads Per Hour.

Absorbed Dose (Mrads)	Dielectric Constant				Dissipation Factor			
	100 cps	1 kc	10 kc	100 kc	100 cps	1 kc	10 kc	100 kc
6.93	2.126	2.126	2.123	2.123	.0048	.0008	.0002	.0002
7.13	2.126	2.126	2.123	2.123	.0046	.0007	.0002	.0002
7.33	2.126	2.126	2.123	2.123	.0045	.0007	.0002	.0002
7.53	2.126	2.126	2.123	2.123	.0044	.0007	.0002	.0002
7.73	2.126	2.124	2.123	2.123	.0041	.0006	.0002	.0002
7.94	2.126	2.124	2.123	2.123	.0040	.0006	.0002	.0002
8.14	2.126	2.124	2.123	2.123	.0039	.0006	.0002	.0002
8.35	2.126	2.124	2.123	2.123	.0037	.0006	.0002	.0002
8.55	2.126	2.124	2.123	2.121	.0036	.0006	.0002	.0002
9.90	2.124	2.124	2.123	2.121	.0034	.0005	.0002	.0002
10.3	2.124	2.124	2.123	2.121	.0032	.0005	.0002	.0002
11.78	2.124	2.124	2.123	2.121	.0020	.0004	.0002	.0002
12.38	2.124	2.124	2.123	2.121	.0014	.0004	.0002	.0002
13.45	2.124	2.124	2.123	2.121	.0010	.0002	.0002	.0002
17.25	2.124	2.124	2.123	2.121	.0005	.0002	.0002	.0002
26.35	2.124	2.124	2.123	2.121	.0005	.0002	.0002	.0002

Table III. FEP-100 Recovery Data.

A. Absorbed Dose = 10.3 Mrads.
Recovery in Vacuum.

Recovery Time (Hours)	Dielectric Constant				Dissipation Factor (Values multiplied by 10^4)			
	100 cps	1 kc	10 kc	100 kc	100 cps	1 kc	10 kc	100 kc
0	2.124	2.124	2.123	2.121	32	5	2	2
1	2.124	2.124	2.123	2.121	10	5	2	2
2	2.124	2.124	2.123	2.121	8	3	5	2
4	2.124	2.124	2.123	2.121	6	3	8	2
23	2.124	2.124	2.123	2.121	5	3	2	2
28	2.124	2.124	2.123	2.121	5	3	2	2
96	2.124	2.124	2.123	2.121	4	2	2	2

Cell vented to helium. No effect on dielectric constant or dissipation factor after 4 hours.

B. Absorbed Dose = 26.35 Mrads.

Recovery Time (Hours)	Dielectric Constant				Dissipation Factor (Values multiplied by 10^4)			
	100 cps	1 kc	10 kc	100 kc	100 cps	1 kc	10 kc	100 kc
0	2.124	2.124	2.123	2.121	5	2	2	2
1	2.124	2.124	2.123	2.121	4	2	2	2
2	2.124	2.124	2.123	2.121	4	2	2	2
24	2.124	2.124	2.123	2.121	4	2	2	2
*25	2.124	2.124	2.123	2.121	8	4	4	2
25.5	2.124	2.124	2.123	2.121	9	3	4	2
28	2.124	2.124	2.123	2.121	8	3	3	2
31	2.124	2.124	2.123	2.121	4	2	3	2
48	2.124	2.124	2.123	2.121	4	2	2	2
168	2.121	2.121	2.119	2.119	4	2	2	2

* Cell vented to room air after 24 hours. Remainder of recovery in air.

Table IV. PF Vacuum X-Ray Exposure Data; Dose Rate 0.2 Mrads Per Hour.

Absorbed Dose (Mrads)	Dielectric Constant				Dissipation Factor			
	100 cps	1 kc	10 kc	100 kc	100 cps	1 kc	10 kc	100 kc
0	2.082	2.082	2.078	2.076	.0004	.0003	.0002	.0002
.20	2.082	2.082	2.078	2.076	.0004	.0003	.0002	.0002
.51	2.082	2.082	2.078	2.076	.0004	.0003	.0002	.0002
.81	2.082	2.082	2.078	2.076	.0004	.0003	.0002	.0002
1.21	2.082	2.082	2.078	2.076	.0005	.0003	.0002	.0002
1.62	2.082	2.082	2.078	2.076	.0006	.0003	.0002	.0002
2.03	2.082	2.082	2.078	2.076	.0010	.0003	.0002	.0002
2.43	2.082	2.082	2.078	2.076	.0012	.0003	.0003	.0002
2.63	2.082	2.082	2.078	2.076	.0014	.0003	.0003	.0002
2.83	2.082	2.082	2.078	2.076	.0016	.0003	.0003	.0003
3.03	2.082	2.082	2.078	2.076	.0018	.0003	.0003	.0003
3.23	2.082	2.082	2.078	2.076	.0021	.0003	.0003	.0003
3.34	2.082	2.082	2.078	2.076	.0024	.0004	.0003	.0003
3.64	2.082	2.082	2.078	2.076	.0030	.0005	.0003	.0003
3.74	2.082	2.082	2.078	2.076	.0030	.0005	.0003	.0003
4.45	2.084	2.082	2.078	2.076	.0059	.0008	.0003	.0003
5.06	2.086	2.082	2.078	2.076	.0102	.0014	.0003	.0003
5.54	2.088	2.082	2.078	2.076	.0120	.0024	.0004	.0003
6.06	2.091	2.082	2.078	2.076	.0165	.0029	.0005	.0004
6.87	2.095	2.082	2.078	2.076	.0228	.0034	.0005	.0004
7.28	2.097	2.082	2.080	2.078	.0260	.0039	.0006	.0004
7.69	2.101	2.082	2.082	2.080	.0291	.0043	.0006	.0004
8.29	2.103	2.086	2.082	2.080	.0354	.0053	.0007	.0004
8.49	2.105	2.088	2.082	2.080	.0386	.0056	.0008	.0004
9.70	2.110	2.090	2.082	2.082	.0503	.0070	.0010	.0004
10.90	2.120	2.090	2.084	2.082	.0595	.0083	.0012	.0004
11.70	2.124	2.092	2.084	2.084	.0644	.0094	.0013	.0004
12.12	2.126	2.092	2.084	2.084	.0649	.0096	.0014	.0006
16.95	2.134	2.097	2.088	2.088	.0732	.0107	.0016	.0006
21.25	2.137	2.101	2.091	2.088	.0673	.0101	.0016	.0006
22.25	2.134	2.097	2.091	2.088	.0629	.0097	.0015	.0006

Table V. PF Vacuum X-Ray Recovery Data.

A. Recovery in Vacuum.

Recovery Time (Hours)	Dielectric Constant				Dissipation Factor			
	100 cps	1 kc	10 kc	100 kc	100 cps	1 kc	10 kc	100 kc
0	2.134	2.097	2.091	2.088	.0629	.0097	.0015	.0006
1.5	2.128	2.097	2.091	2.088	.0580	.0086	.0014	.0005
3.5	2.126	2.097	2.091	2.088	.0513	.0076	.0012	.0005
19	2.112	2.097	2.091	2.088	.0297	.0046	.0008	.0006
21	2.110	2.097	2.091	2.088	.0283	.0043	.0007	.0006
27	2.110	2.097	2.091	2.088	.0274	.0042	.0007	.0006
43	2.108	2.097	2.091	2.088	.0230	.0036	.0006	.0006
51	2.108	2.097	2.091	2.088	.0216	.0034	.0006	.0006
67	2.105	2.097	2.091	2.088	.0178	.0028	.0005	.0005
99	2.101	2.097	2.091	2.088	.0133	.0021	.0003	.0004

B. Recovery in Vacuum for 24 Hours.
Remainder of Recovery in Nitrogen at Atmospheric Pressure.

Recovery Time (Hours)	Dielectric Constant				Dissipation Factor			
	100 cps	1 kc	10 kc	100 kc	100 cps	1 kc	10 kc	100 kc
0	2.134	2.097	2.091	2.088	.0629	.0097	.0015	.0006
24	2.110	2.097	2.091	2.088	.0283	.0043	.0007	.0006
25	2.120	2.099	2.093	2.091	.0239	.0042	.0008	.0006
26	2.135	2.102	2.095	2.093	.0257	.0081	.0011	.0008
29	2.143	2.109	2.101	2.095	.0642	.0172	.0026	.0008
48	2.175	2.115	2.103	2.101	.161	.0250	.0035	.0010
54	2.190	2.117	2.105	2.101	.183	.0280	.0039	.0010
72	2.155	2.107	2.095	2.093	.189	.0268	.0036	.0006
80	2.155	2.107	2.093	2.091	.186	.0268	.0036	.0005
96	2.143	2.107	2.093	2.091	.165	.0254	.0032	.0004
168	2.130	2.105	2.093	2.091	.136	.0188	.0025	.0003

Table VI. K-4 Vacuum X-Ray Exposure and Vacuum Recovery Data; Dose Rate 0.7 Mrads Per Hour.

Absorbed Dose (Mrads)	Dielectric Constant				Dissipation Factor			
	100 cps	1 kc	10 kc	100 kc	100 cps	1 kc	10 kc	100 kc
0	2.751	2.661	2.555	2.477	.0176	.0262	.0249	.0168
.70	2.756	2.667	2.560	2.481	.0180	.0263	.0254	.0173
1.40	2.706	2.673	2.564	2.482	.0176	.0263	.0260	.0179
2.10	2.765	2.677	2.567	2.484	.0176	.0264	.0271	.0183
2.44	2.768	2.681	2.570	2.486	.0176	.0264	.0264	.0185
3.49	2.773	2.687	2.574	2.489	.0174	.0264	.0269	.0188
4.18	2.777	2.690	2.578	2.490	.0173	.0264	.0271	.0189
4.88	2.780	2.695	2.581	2.492	.0170	.0263	.0273	.0192
5.58	2.784	2.699	2.585	2.495	.0169	.0263	.0277	.0196
16.45	2.796	2.713	2.598	2.505	.0163	.0261	.0284	.0203
18.15	2.796	2.713	2.596	2.503	.0161	.0259	.0283	.0206
18.85	2.796	2.713	2.596	2.503	.0160	.0259	.0283	.0206
20.25	2.797	2.715	2.599	2.505	.0159	.0259	.0283	.0207
21.65	2.798	2.717	2.602	2.506	.0156	.0257	.0283	.0206
33.20	2.798	2.718	2.603	2.506	.0155	.0255	.0284	.0199
35.0	2.798	2.717	2.602	2.507	.0153	.0255	.0284	.0220
Recovery Time (Hours)								
1.0	2.791	2.711	2.597	2.504	.0152	.0254	.0281	.0205
2.5	2.785	2.705	2.592	2.502	.0155	.0254	.0274	.0200
6.0	2.780	2.697	2.586	2.498	.0156	.0257	.0271	.0190
28.5	2.761	2.678	2.572	2.489	.0161	.0254	.0258	.0187
84.5	2.760	2.676	2.570	2.488	.0163	.0254	.0256	.0184
113.5	2.760	2.677	2.570	2.489	.0160	.0253	.0256	.0184

Table VII. Effect of Voltage Application Time on the Electric Strength of Polystyrene; Breakdown Thickness 10-mils.

Specimen	Frequency	Stress (rms KV/mil)	Time (seconds)	Remarks
1	60 cps	6.0	2	Withstand
1	60 cps	4.1	180	Puncture
2	1 kc	4.5	60	Puncture*
3	38 kc	3.1	180	Puncture
4	38 kc	3.5	300	Withstand*
5	2 mc	2.7	$\approx$0.1	Withstand
6	2 mc	1.7	3	Puncture
7	2 mc	1.0	15	Deformation
8	5 mc	1.0	3	Puncture
9	5 mc	0.6	90	Deformation
10	18 mc	1.0	<0.1	Withstand
10	18 mc	1.0	0.5	Puncture
11	18 mc	0.3	300	Deformation

* Maximum Available Voltage.

Table VIII. Percentage Decrease from 25°C Values of Capacitance of FEP-100 Specimens. Rate of Temperature Rise 0.7°C Per Minute.

Temp. (°C)	100 cps	1 kc	10 kc	100 kc	1 mc	3 mc	10 mc	30 mc
30	0	0	0	0	0	0	0.1	0.1
35					0.1	0.1	0.2	0.2
40	0.2	0.2	0.2	0.2	0.2	0.2	0.3	0.3
45					0.2	0.2	0.5	0.5
50	0.4	0.4	0.5	0.5	0.5	0.4	0.7	0.7
55					0.5	0.5	0.9	0.9
60	1.1	1.1	1.2	1.3	0.7	0.7	1.1	1.1
65					1.0	1.0	1.4	1.4
70	2.1	2.1	2.1	2.1	1.3	1.3	1.8	1.8
75					1.8	1.8	2.2	2.2
80	3.0	3.0	3.1	3.1	2.0	2.2	2.6	2.6
85					2.5	2.7	3.1	3.1
90	3.5	3.5	3.6	3.7	3.5	3.2	3.6	3.6
95					3.7	3.6	4.1	4.1
100	4.1	4.1	4.2	4.3	4.3	4.3	4.6	4.6
105					4.4	4.4	5.0	5.0
110	4.7	4.7	4.8	4.8	4.8	4.8	5.5	5.5
115					5.2	5.2	5.9	5.9
120	5.4	5.4	5.4	5.4	5.5	5.6	6.2	6.2
125					6.0	6.1	6.6	6.6
130	5.9	5.9	6.0	6.0	6.2	6.5	7.0	7.0
135					6.7	7.0	7.3	7.3
140	6.4	6.4	6.5	6.6	7.0	7.3	7.6	7.6
145					7.6	7.8	7.9	7.9
150	7.1	7.2	7.3	7.4	7.8	8.1	8.2	8.2
155					8.0	8.5	8.6	8.6
160	7.8	7.9	8.0	8.1	8.3	8.8	8.8	8.8
165					8.8	9.2	9.2	9.2
170	8.7	8.8	8.9	9.0	9.3	9.6	9.6	9.6
175					10.0	10.0	10.0	10.0
180	9.7	9.8	9.9	10.2	10.3	10.5	10.5	10.5
185					10.9	10.9	10.9	10.9
190	10.9	11.0	11.1	11.2	11.3	11.3	11.3	11.3
195					11.9	11.8	11.8	11.8
200	12.7	12.8	12.9	13.0	12.5	12.3	12.3	12.3

Table IX. Effect of Temperature on the Dissipation Factor of FEP-100. Rate of Temperature Rise 0.7°C Per Minute.

(All values multiplied by 10^4)

Temp. (°C)	100 cps	1 kc	10 kc	100 kc	1 mc	3 mc	10 mc	30 mc
25	5	5	8	6	5	7	5	8
30	5	5	8	6	5	7	5	8
35					5	7	5	8
40	5	4	7	6	4	6	5	8
45					4	6	5	7
50	6	4	6	7	4	6	5	7
55					3	5	5	6
60	6	4	5	8	3	5	5	6
65					3	5	5	6
70	6	3	4	8	2	5	4	5
75					2	4	4	5
80	6	3	4	9	2	4	4	5
85					2	4	3	5
90	6	3	4	9	2	3	3	5
95					2	3	3	5
100	6	3	3	8	2	3	3	4
105					2	3	3	4
110	6	3	3	7	2	3	3	4
115					2	3	2	4
120	6	3	2	6	2	3	2	4
125					2	3	2	4
130	5	3	2	5	2	3	2	4
135					2	2	2	4
140	5	2	2	4	2	2	2	4
145					1	2	2	4
150	5	2	1	4	1	2	2	3
155					1	2	2	3
160	5	2	1	3	1	2	2	3
165					1	2	2	3
170	6	2	1	2	1	2	2	3
175					1	2	2	3
180	6	2	1	2	1	2	2	3
185					1	2	2	2
190	7	2	1	2	1	2	2	2
195					1	2	2	2
200	7	2	1	2	1	2	2	2

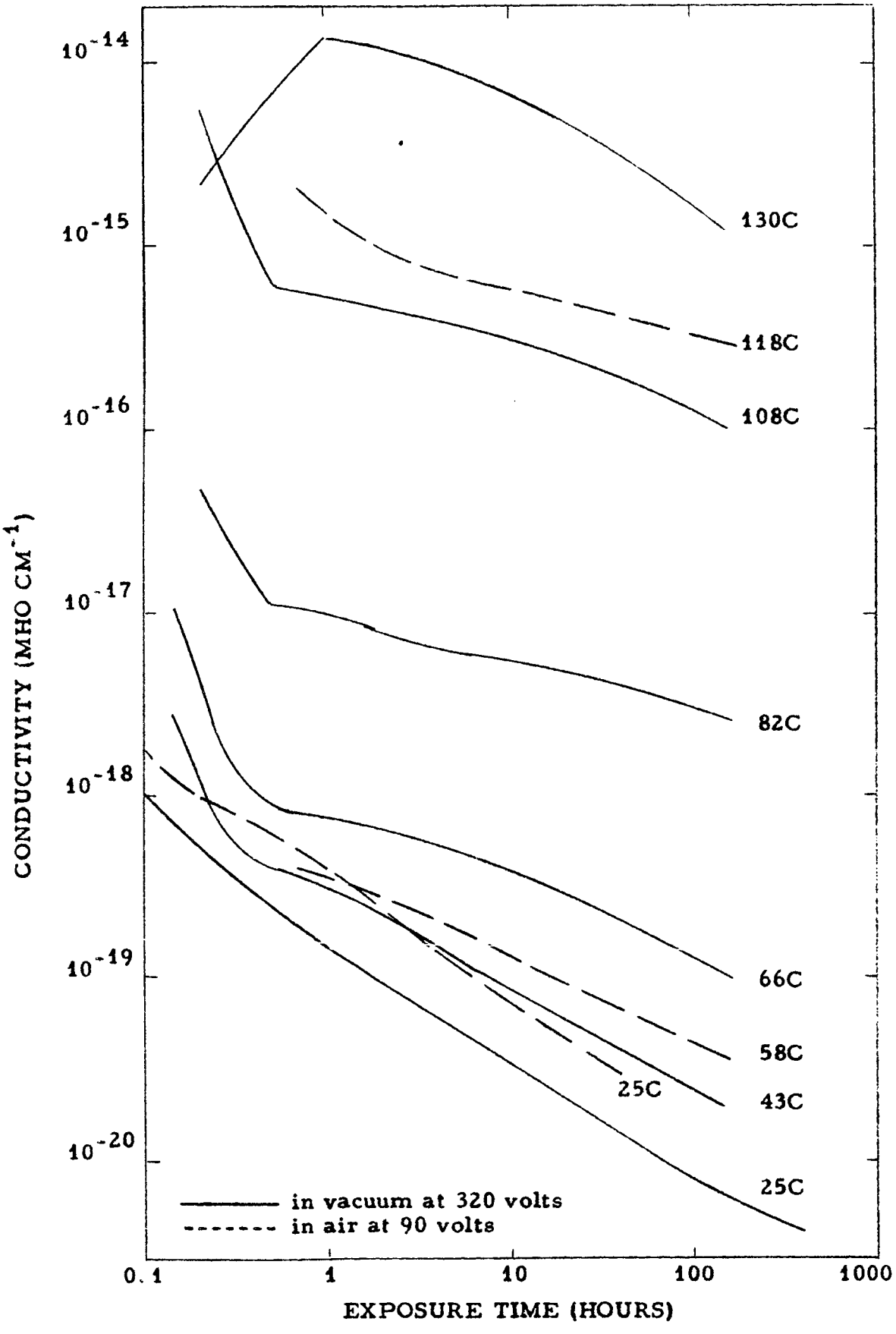

Figure 1. Effect of temperature on conductivity of Mylar Type C 1-mil specimens heated and electrified simultaneously.

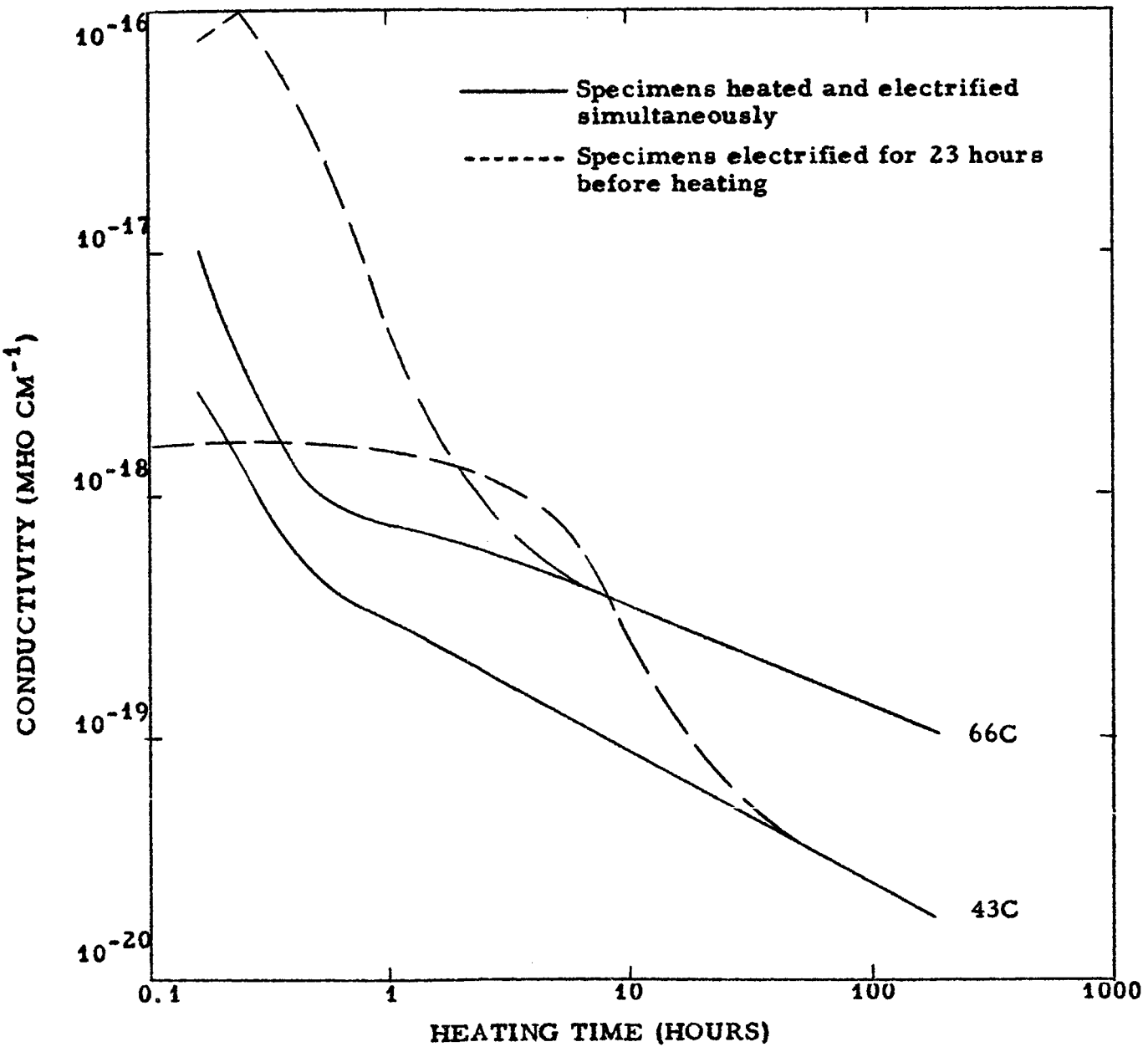

Figure 2. Effect of preheating Mylar Type C conductivity specimens. Applied voltage 320 volts, specimen thickness 1-mil. All exposures in vacuum.

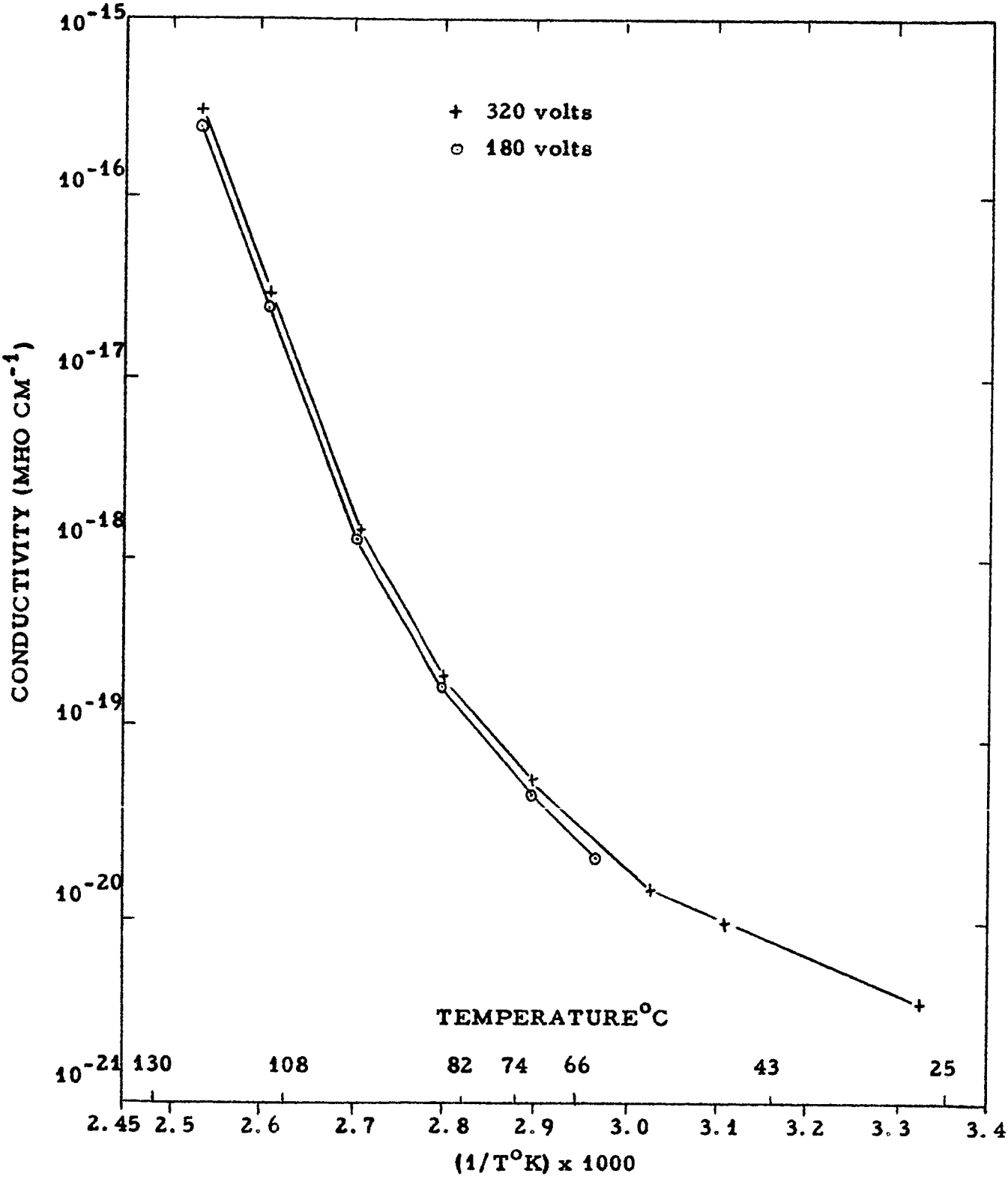

Figure 3. Log σ vs. 1/T for Mylar Type C after 150 hours conditioning at 125°C in vacuum.

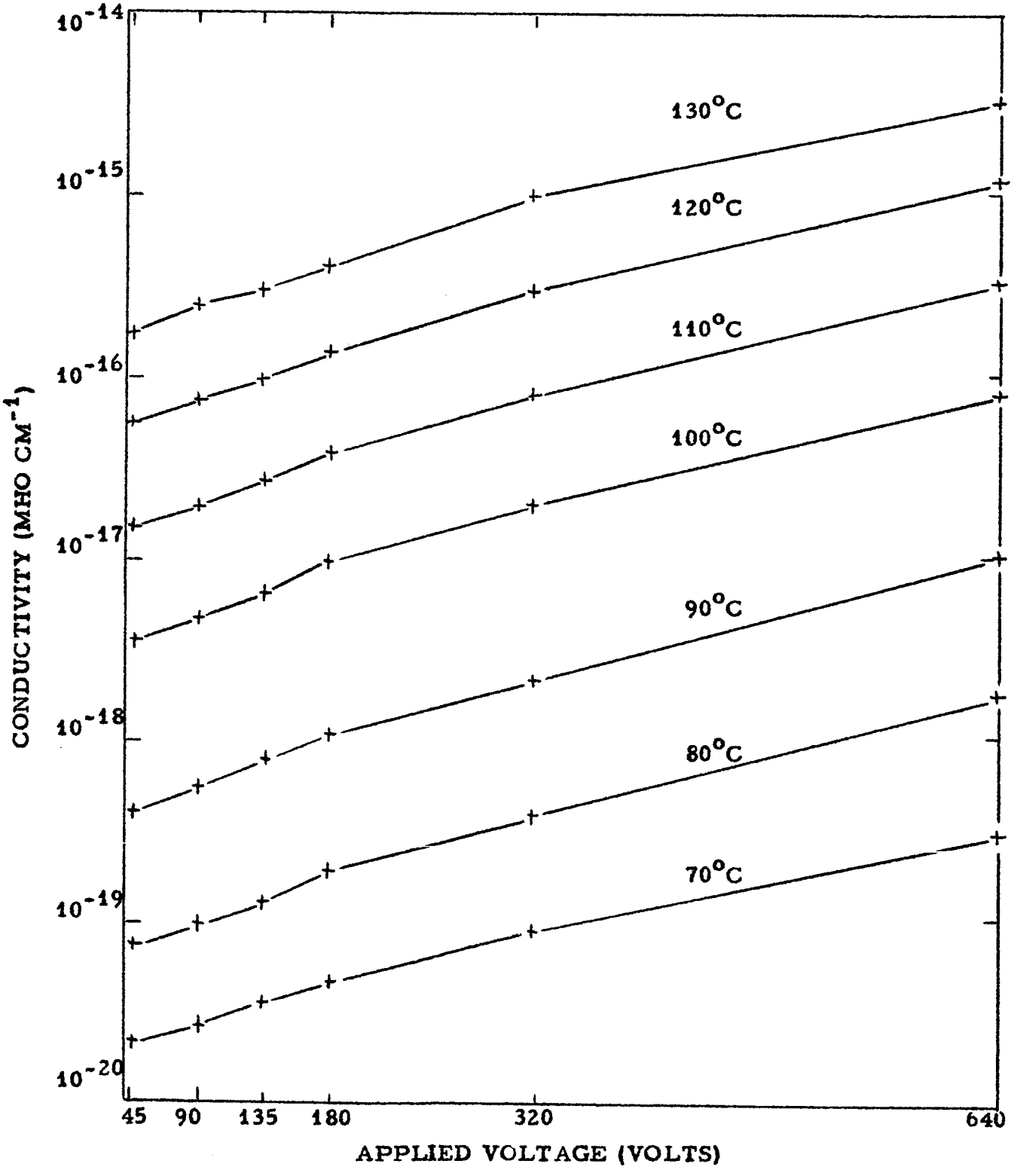

Figure 4. Effect of voltage and temperature on the conductivity of 1-mil Mylar Type C in vacuum.

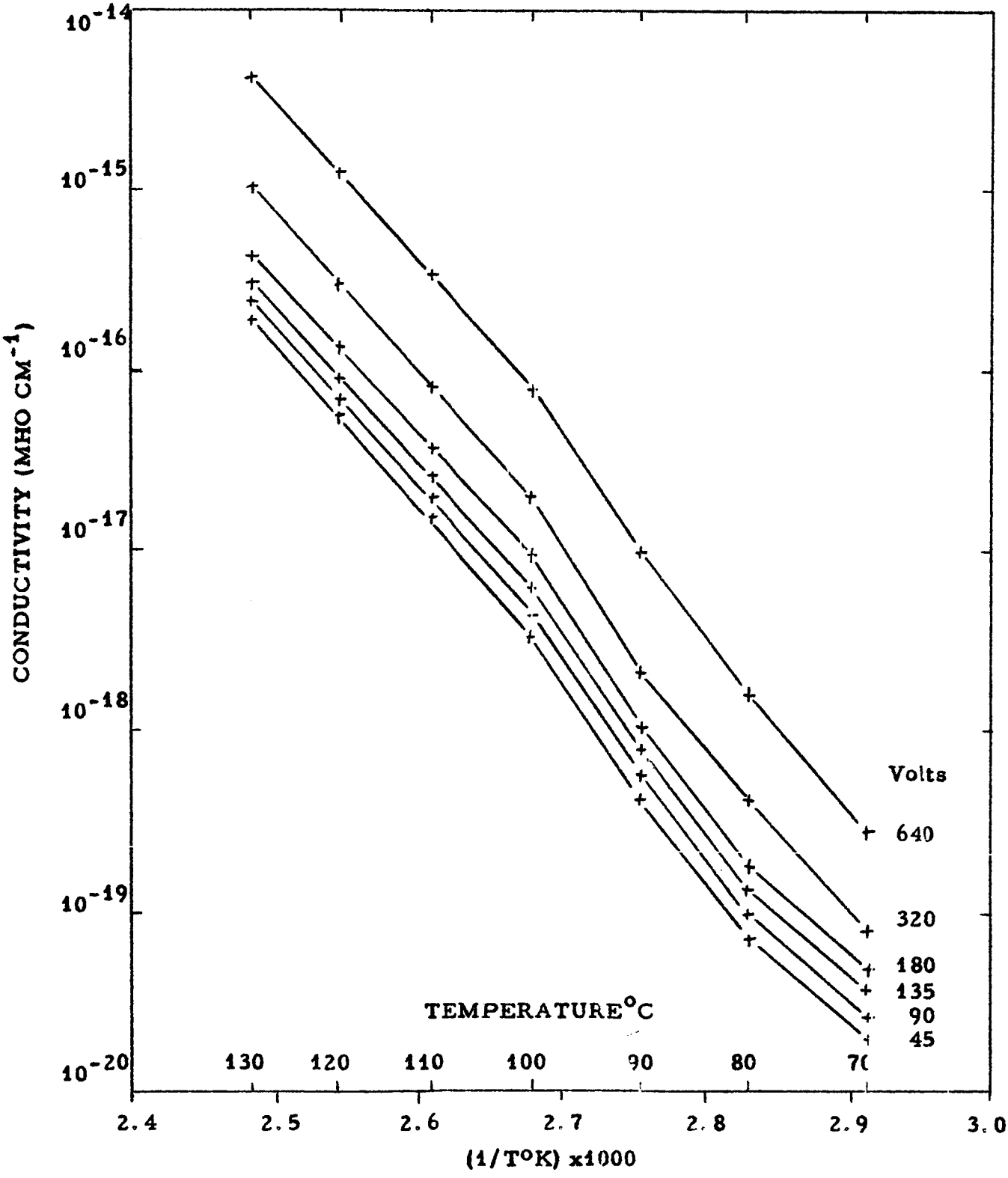

Figure 5. Effect of temperature and voltage on the conductivity of 1-mil Mylar Type C in vacuum.

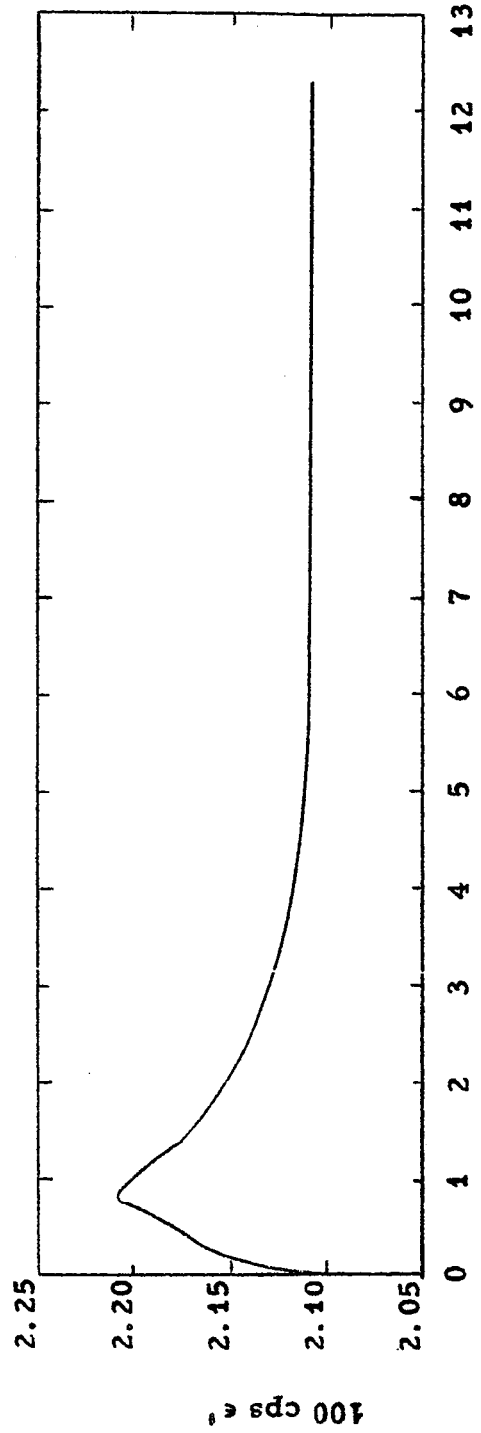

Figure 6. Effect of x-ray irradiation in vacuum on the 100 cps dielectric constant of TFE-7. Specimen thickness 30-mils. Dose rate .025 Mrads/hr.

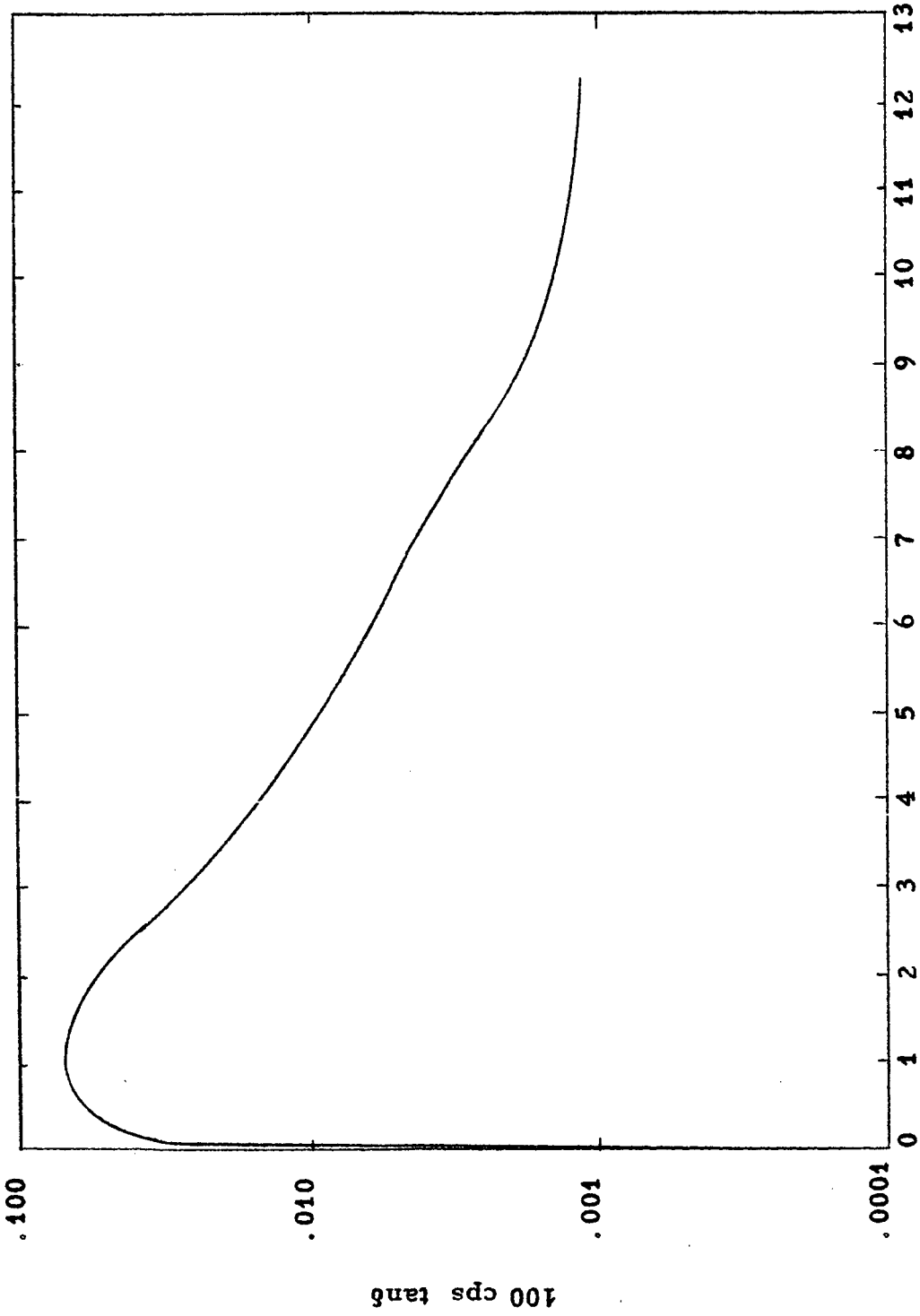

Figure 7. Effect of x-ray irradiation in vacuum on the 100 cps tanδ of TFE-6. Specimen thickness 30-mils. Dose rate .025 Mrads/hr.

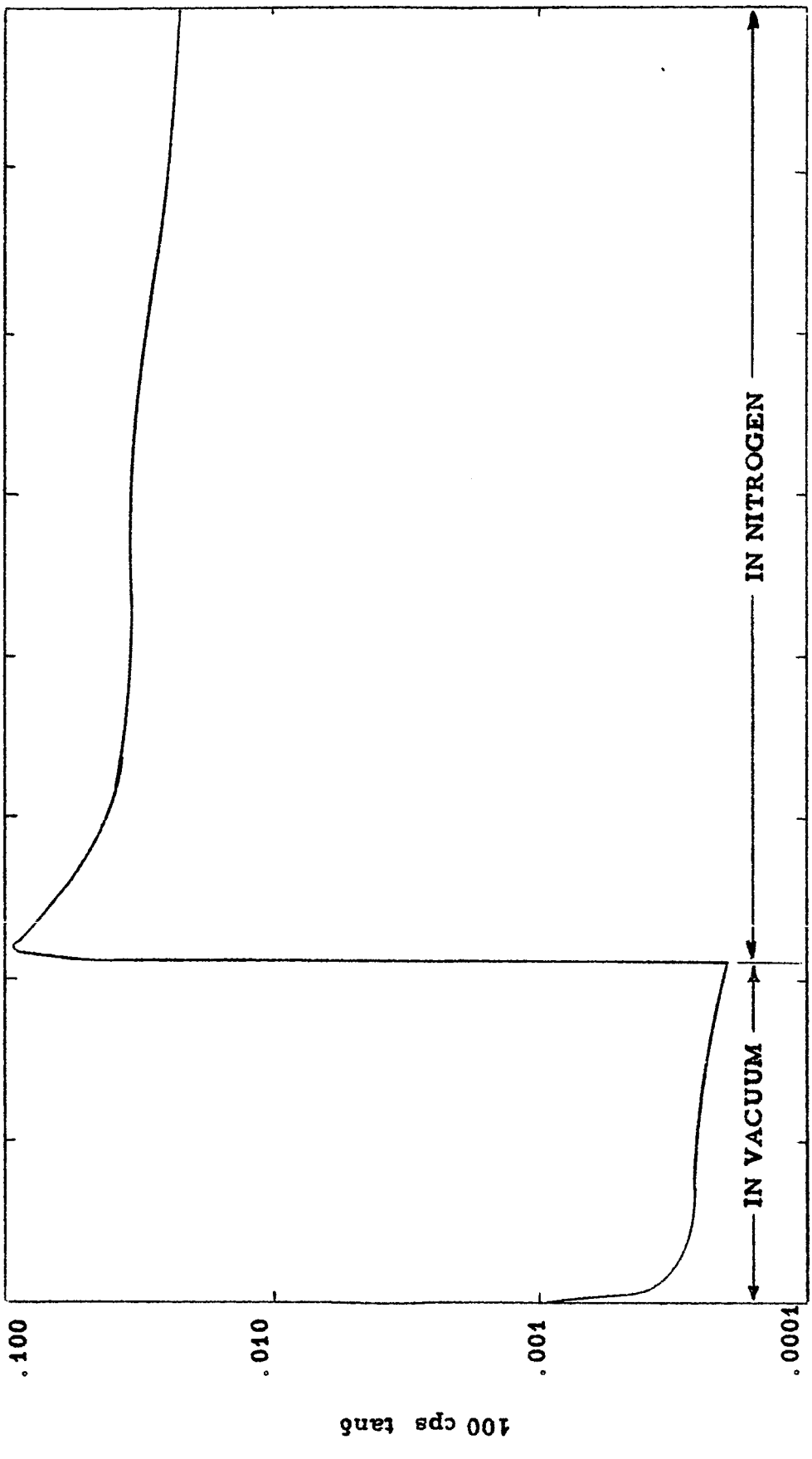

Figure 8. Recovery characteristics of x-ray induced losses in TFE-7

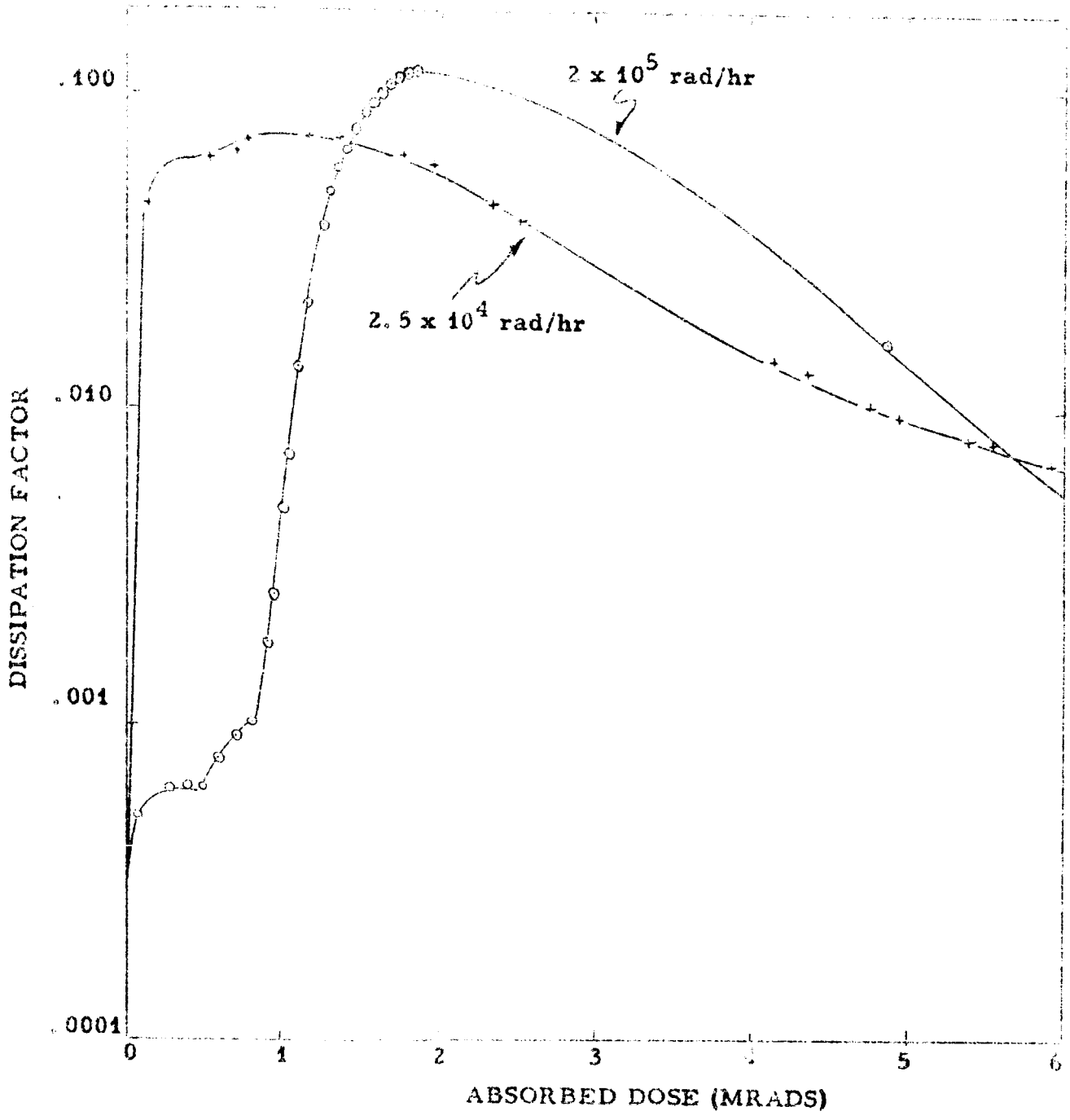

Figure 9. Effect of dose rate on the x-ray induced tanδ of TFE-7 at 100 cps. 30-mil machined specimens exposed in vacuum at room temperature

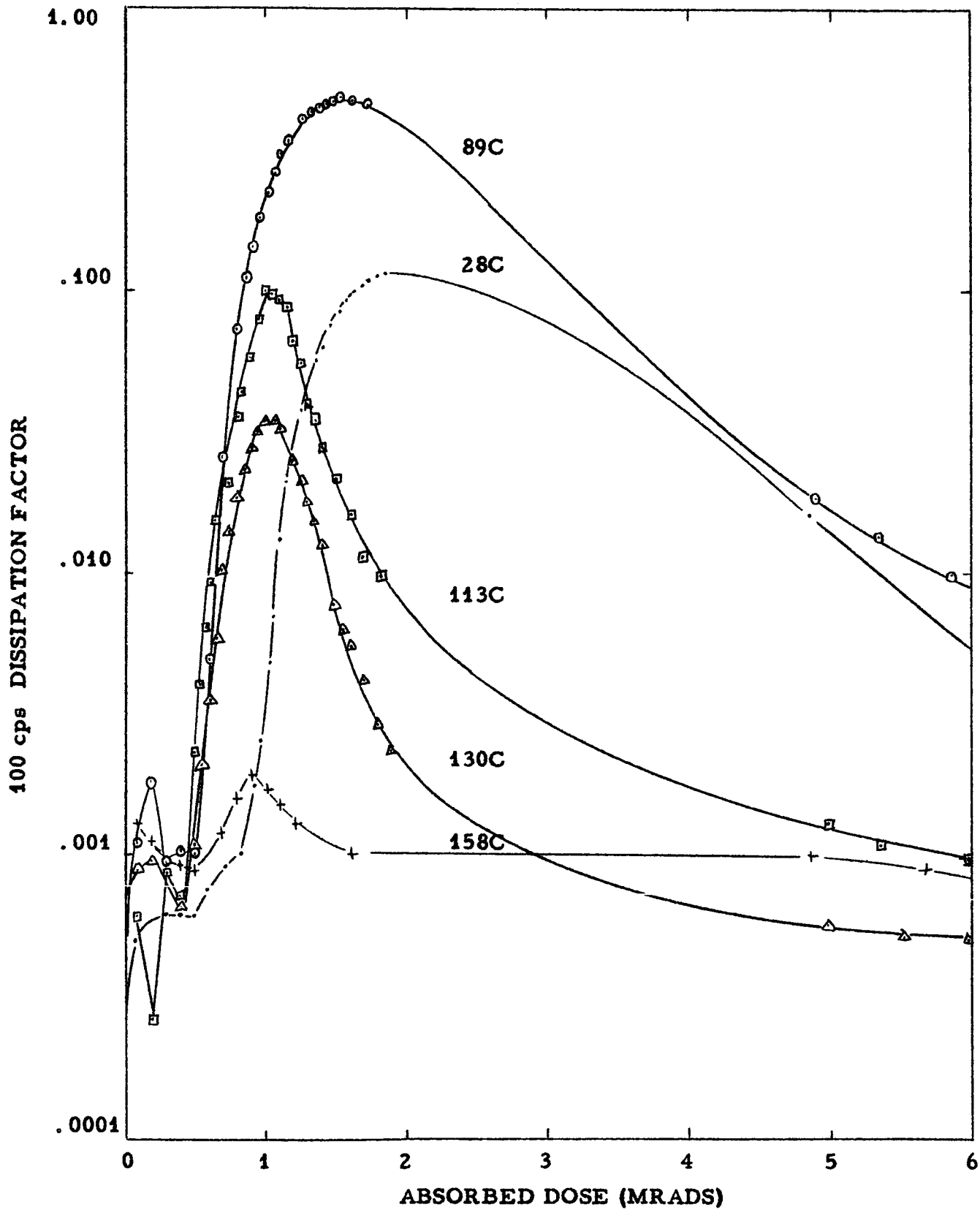

Figure 10. Effect of temperature on the x-ray induced losses in TFE-7 at 100 cps in vacuum. Specimen thickness 30-mils; dose rate 0.2 Mrads per hour.

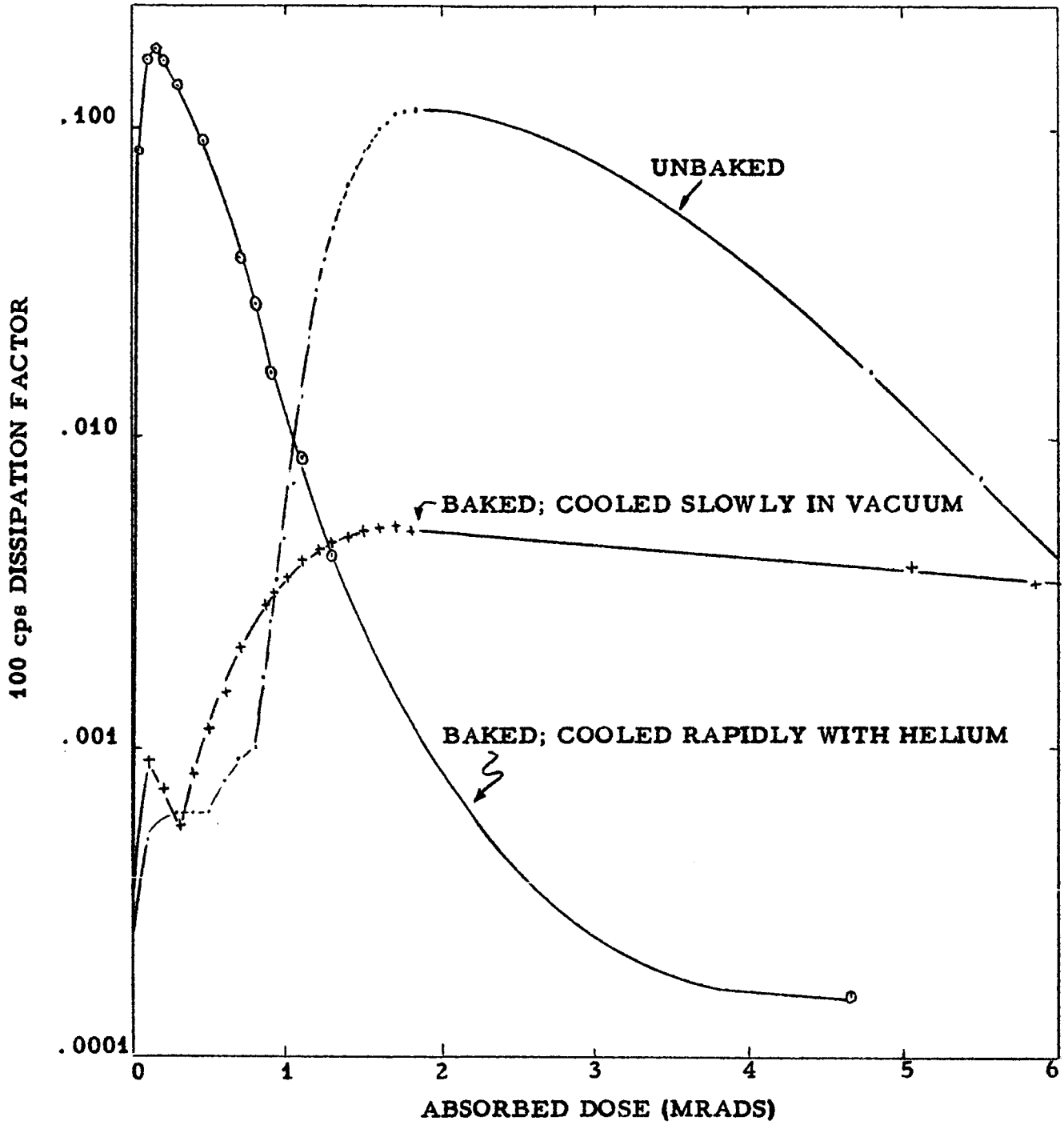

Figure 11. Effect of preconditioning on the x-ray induced losses in TFE-7 at 100 cps. 30-mil machined specimens irradiated in vacuum at room temperature. Dose rate 0.2 Mrads/hr.

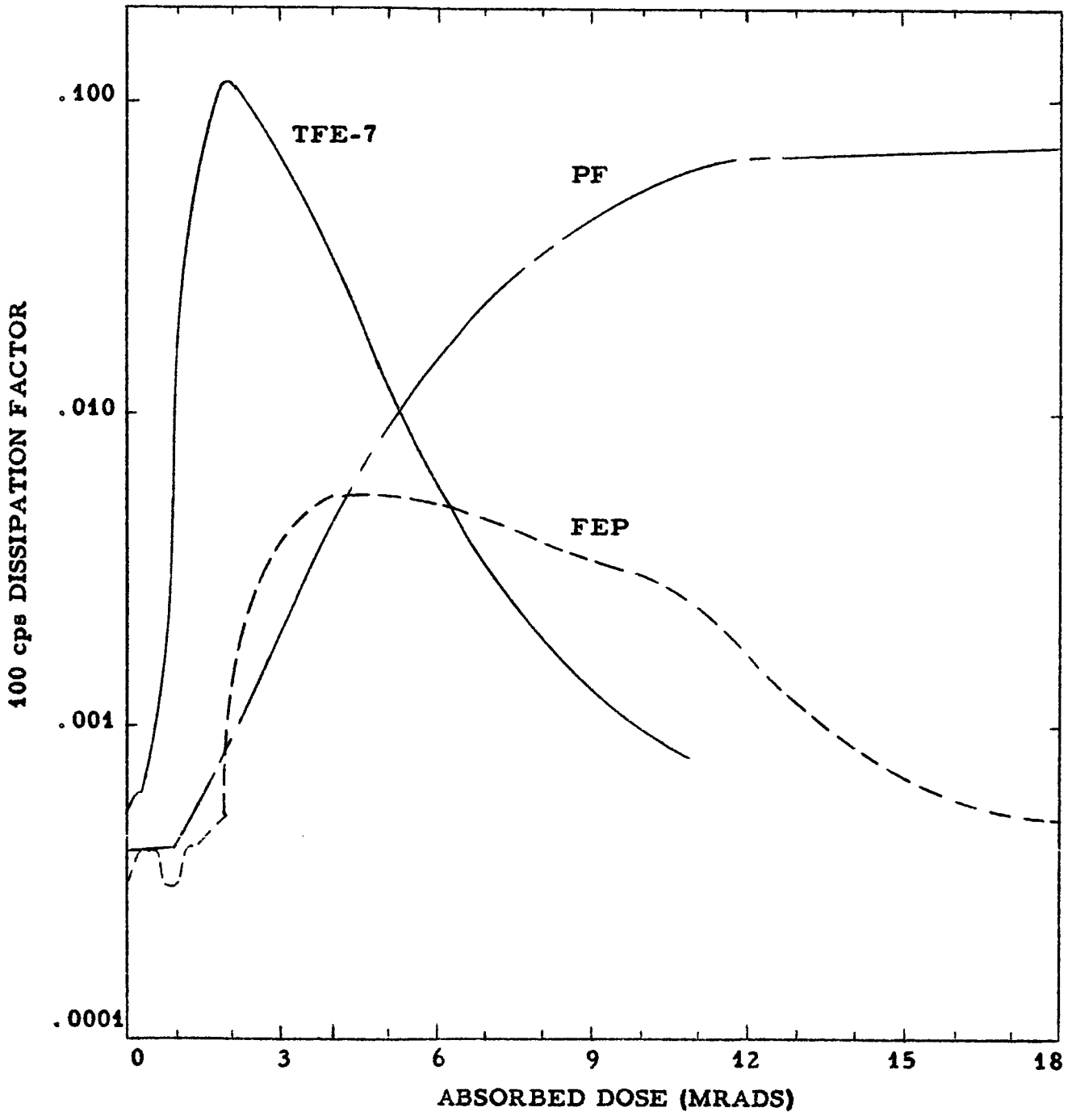

Figure 12. Effect of x-ray irradiation in vacuum on the 100 cps tanδ of TFE-7, FEP-100 and PF. Dose rate 0.2 Mrads/hr.

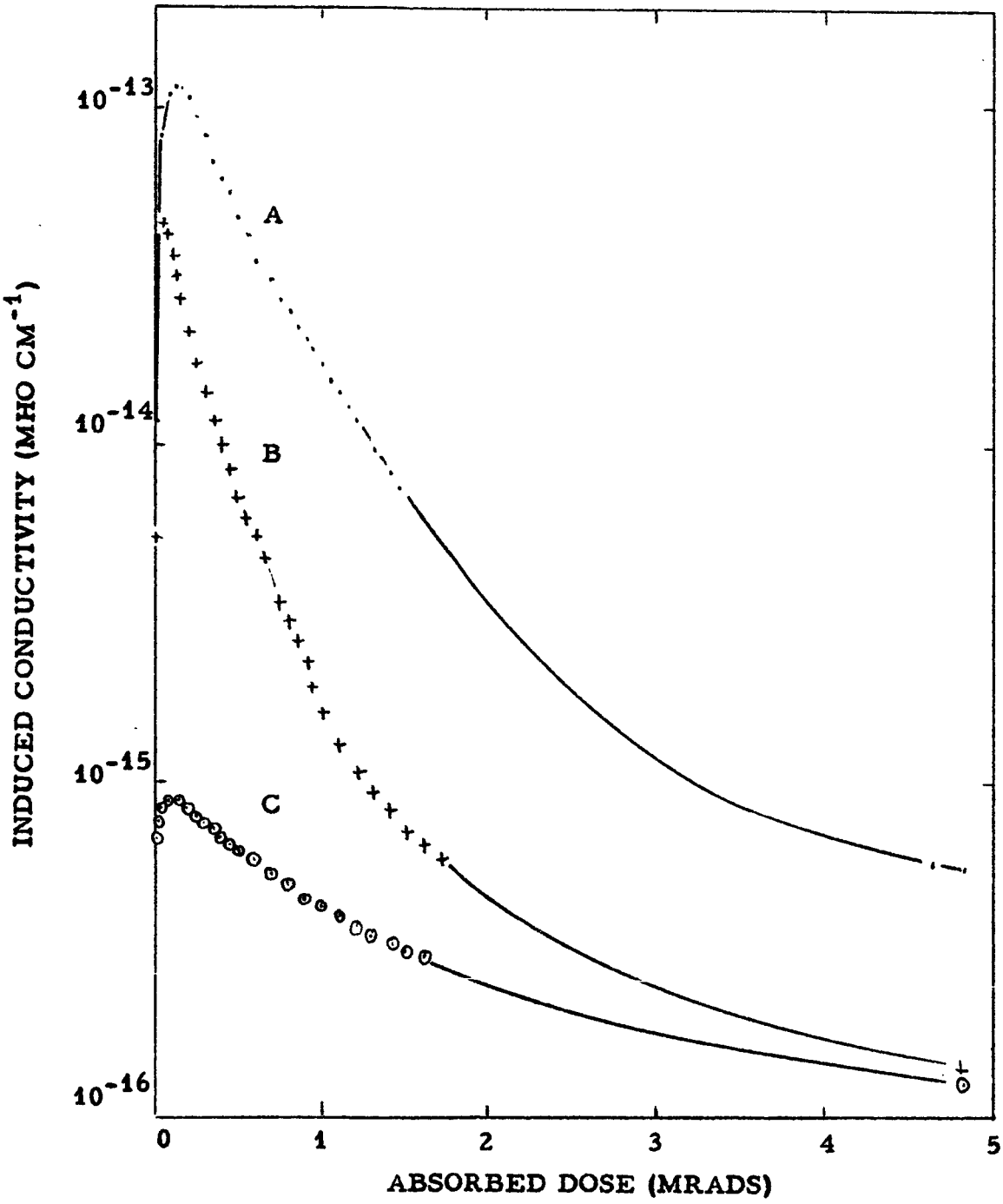

Figure 13. X-ray induced d-c conductivity in 5-mil TFE-7 at room temperature in vacuum. Dose rate 0.20 Mrads/hr. Pre-irradiation treatments: Specimen A - in vacuum at room temperature for 144 hrs.; Specimen B - in vacuum at 165°C for 120 hrs., cooled slowly to room temperature; Specimen C - in vacuum at 166°C for 117 hrs., cooled rapidly to room temperature.

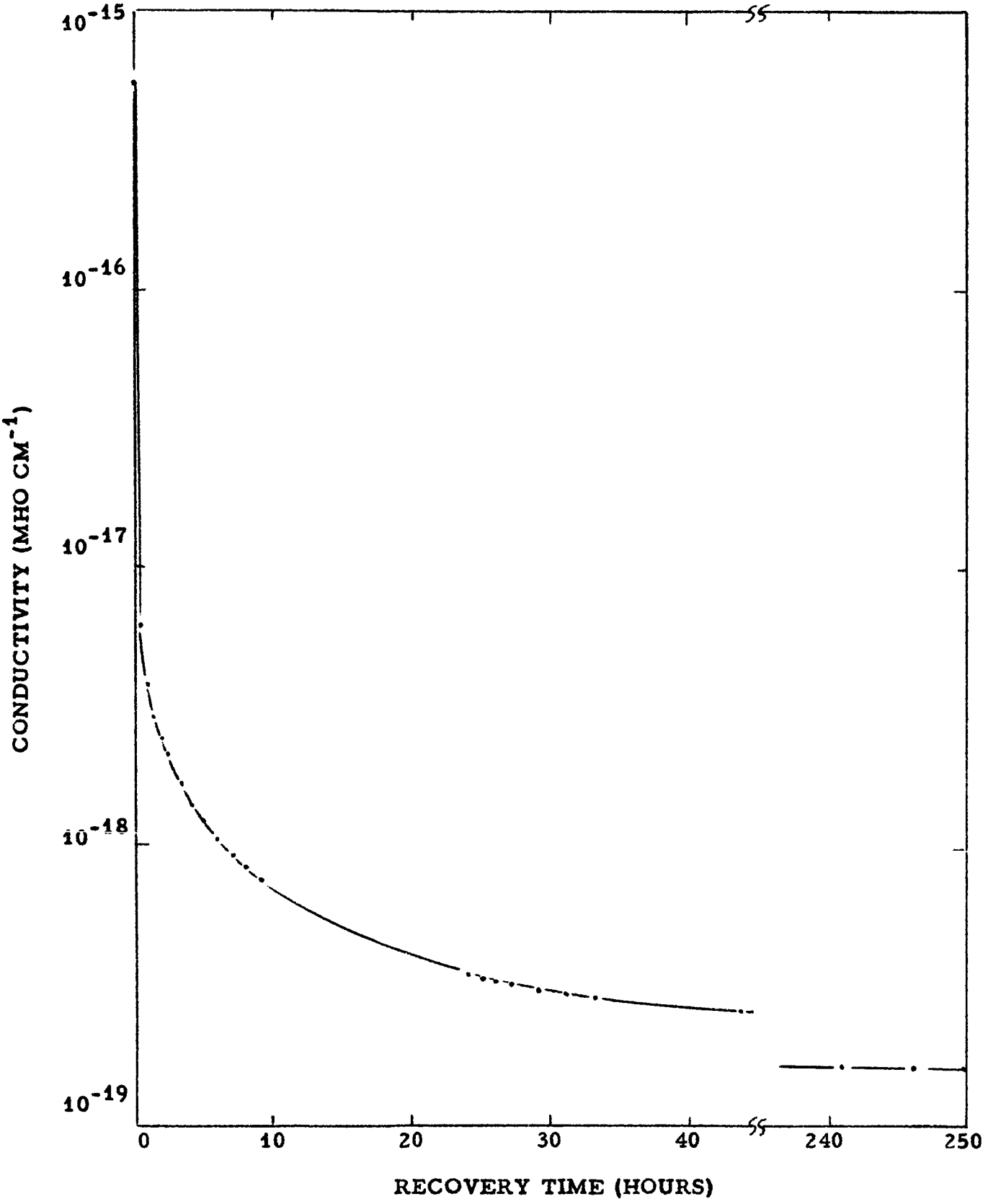

Figure 14. Recovery in vacuum for Specimen A of Figure 13.

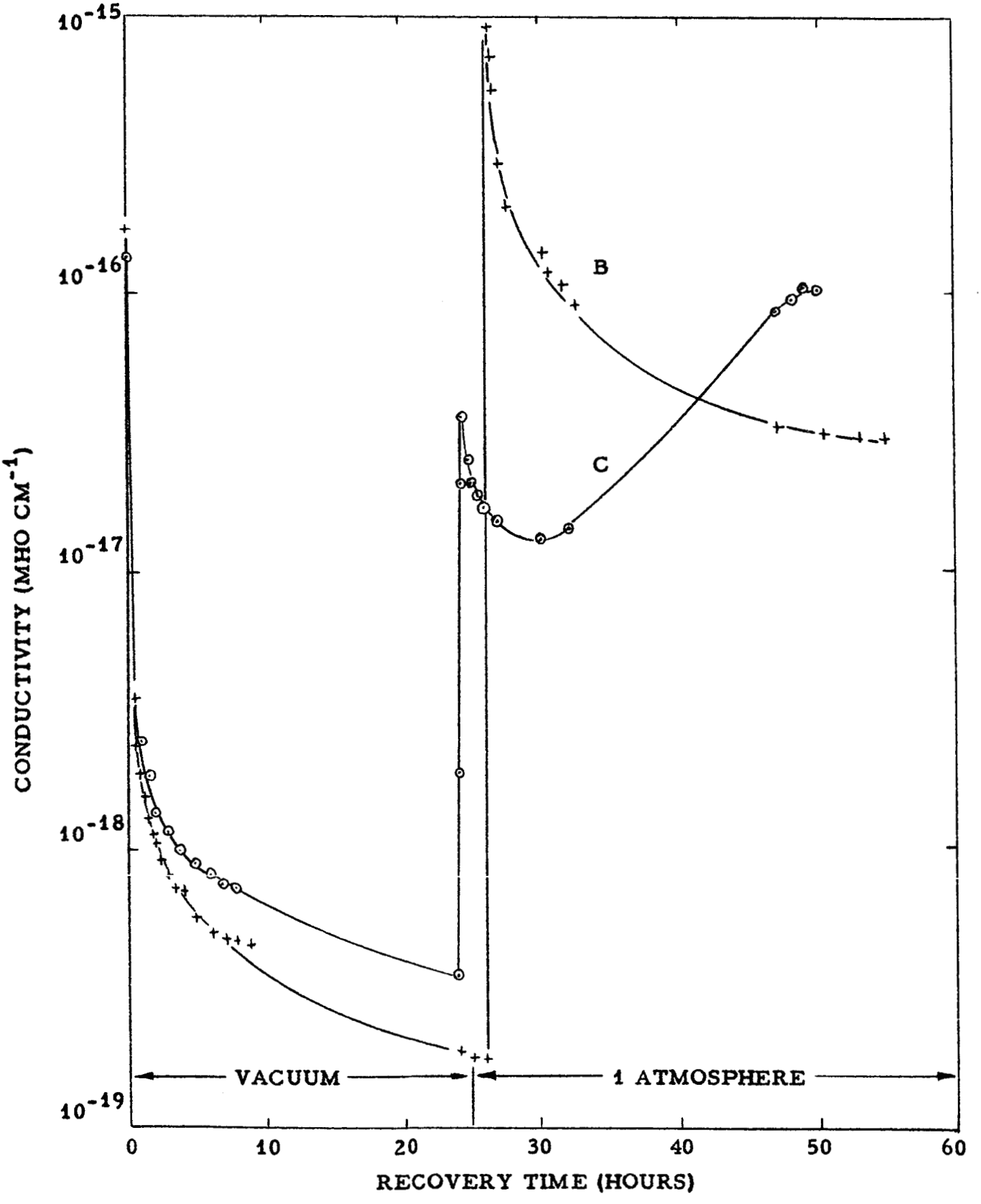

Figure 15. Recovery data for Specimens B and C of Figure 13. Specimen B in vacuum and in air at atmospheric pressure. Specimen C in vacuum and in helium at atmospheric pressure.

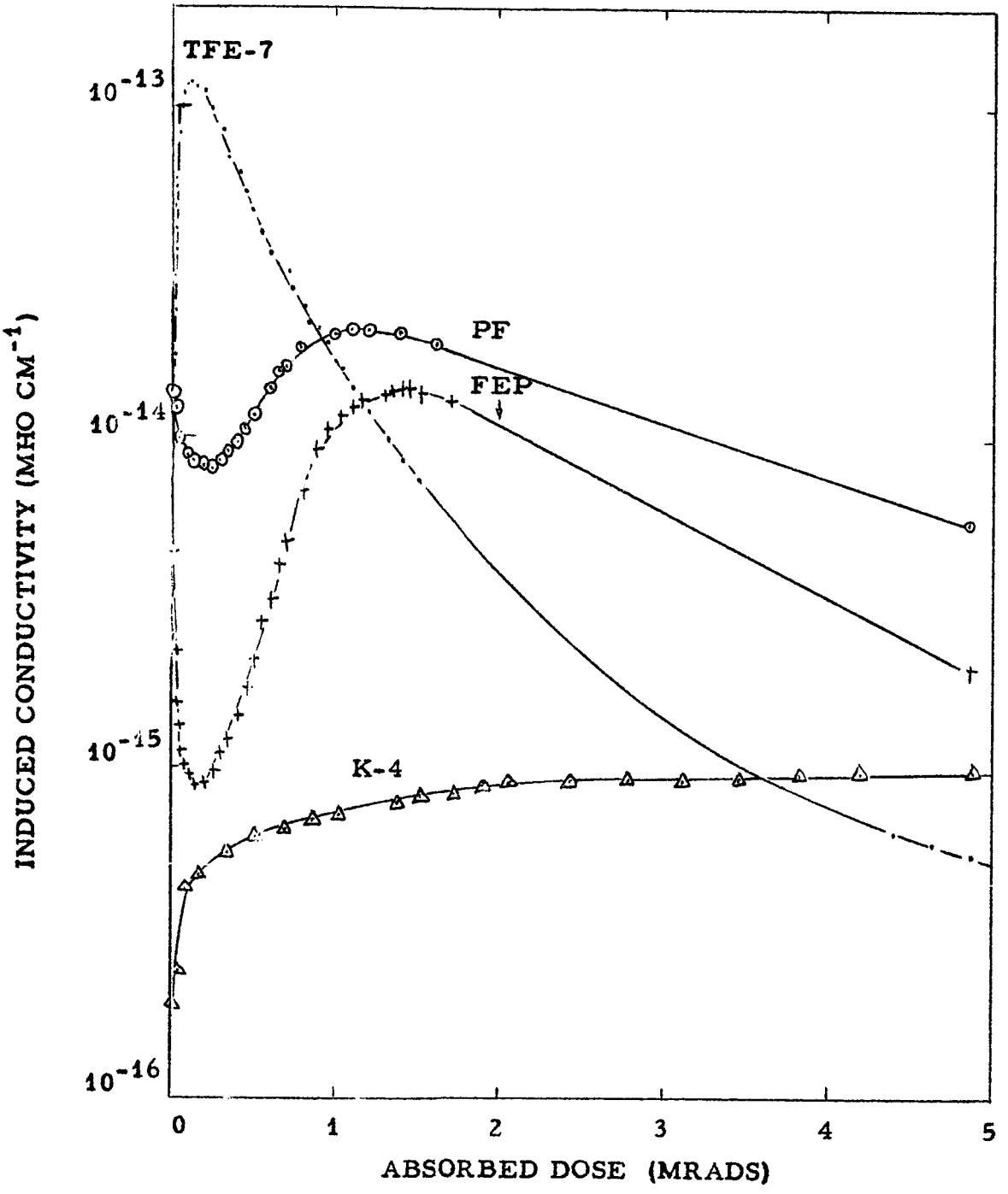

Figure 16. X-ray induced d-c conductivity at room temperature, in vacuum at a dose rate of 0.20 Mrads/hr. for TFE, PF and FEP-100, and at 0.7 Mrads/hr. for K-4.

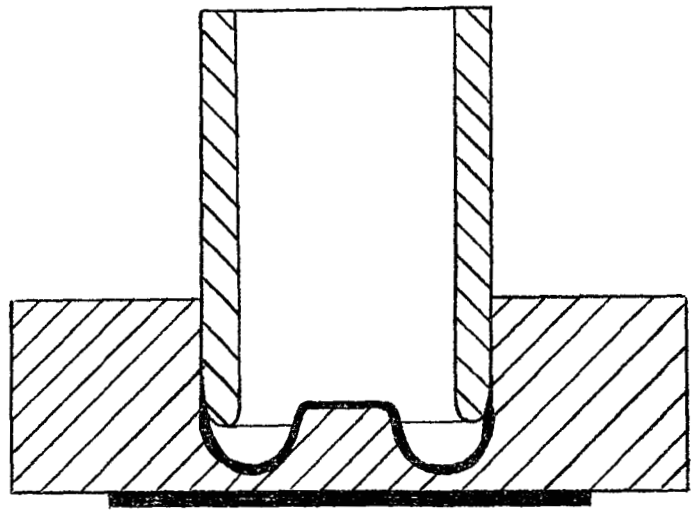

Figure 17. Cross-sectional view of specimen for electric strength measurements at frequencies up to 18 mc (approx. twice full size).

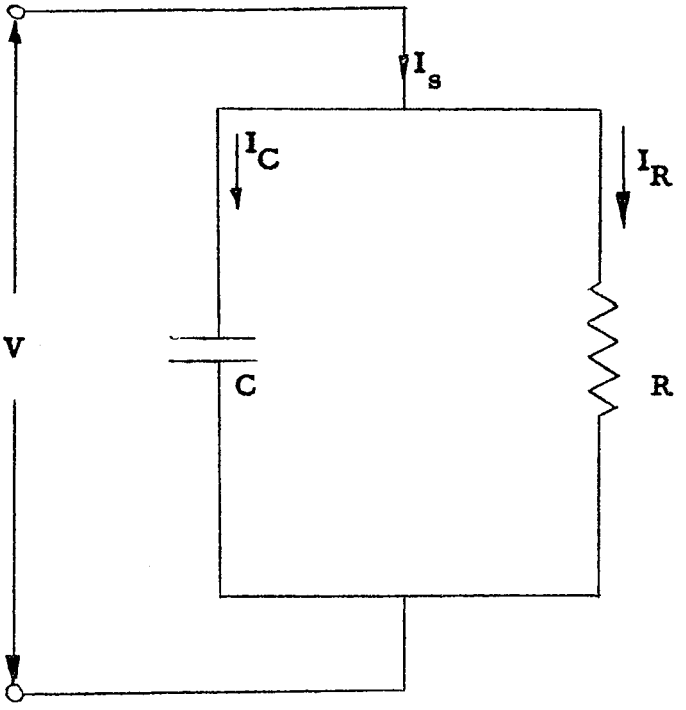

Figure 18. Equivalent circuit of dielectric loss specimen.

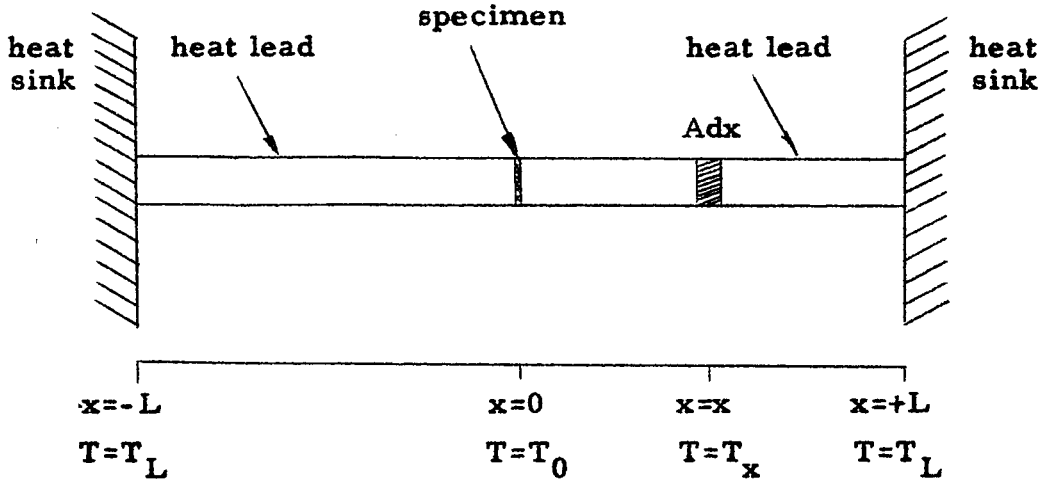

Figure 19. Schematic diagram of calorimeter.

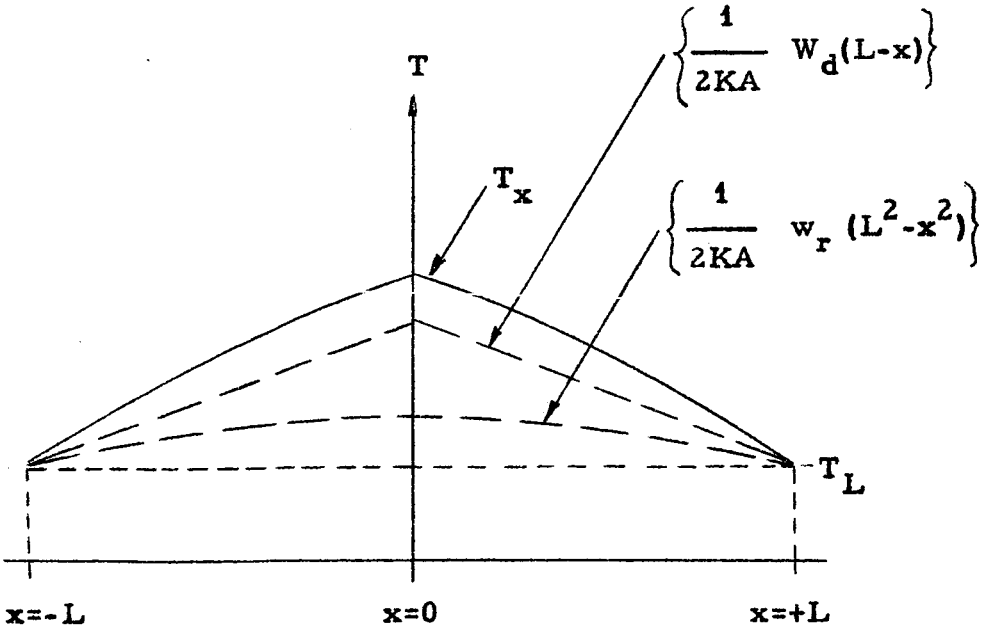

Figure 20. Temperature distribution along heat leads.

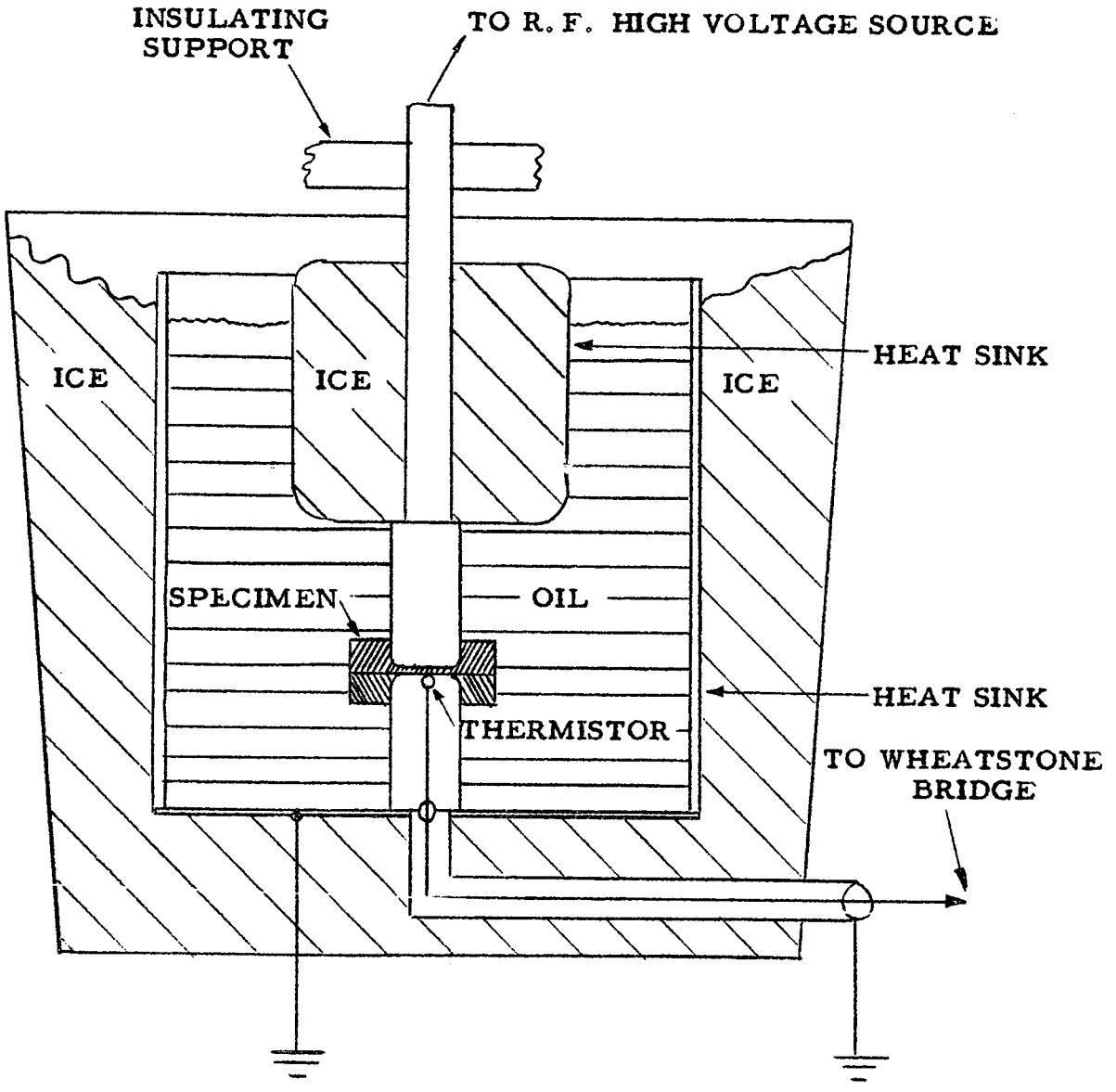

Figure 21. Cross-sectional view of calorimeter (approx. half scale).

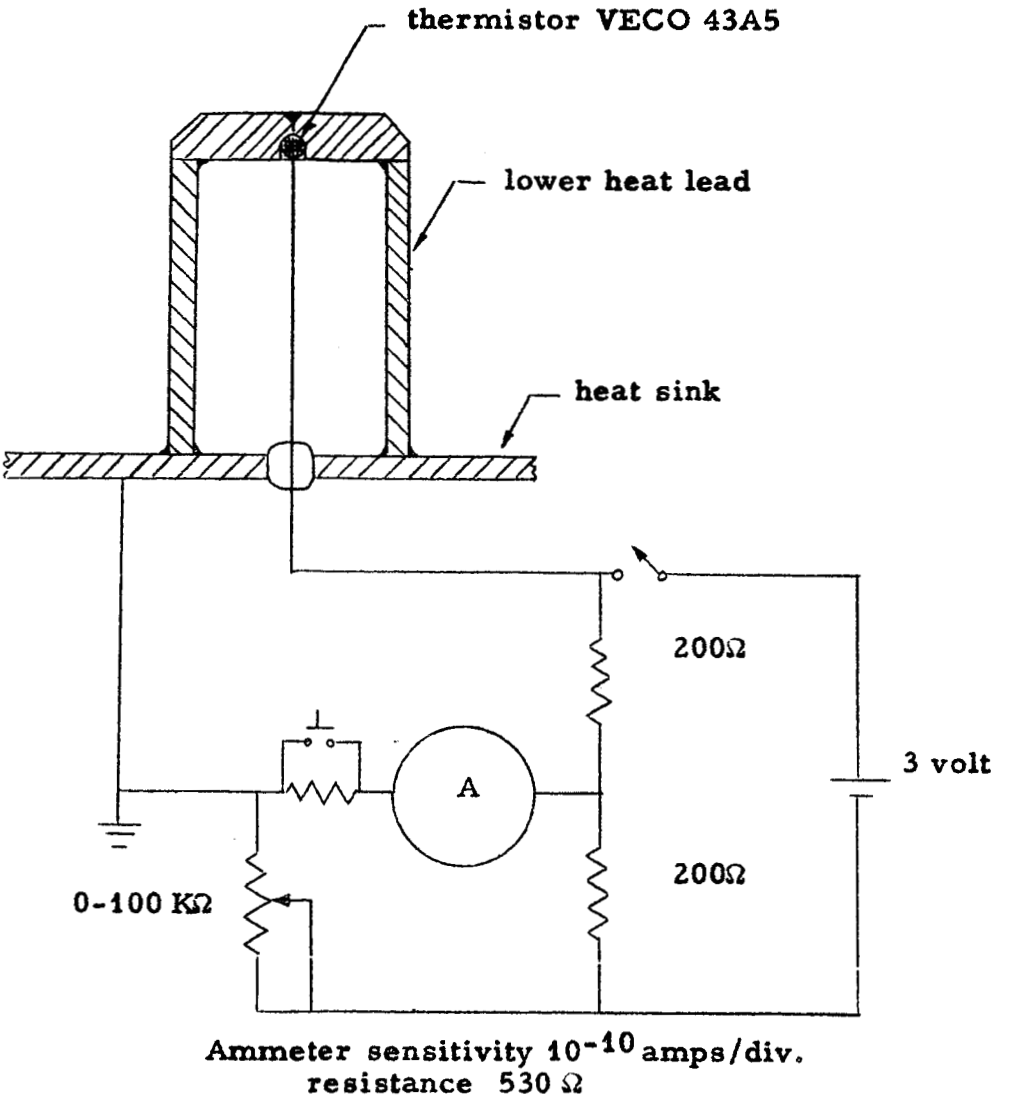

Figure 22. Schematic diagram of temperature measurement circuit. Thermistor resistance measured with Wheatstone Bridge.

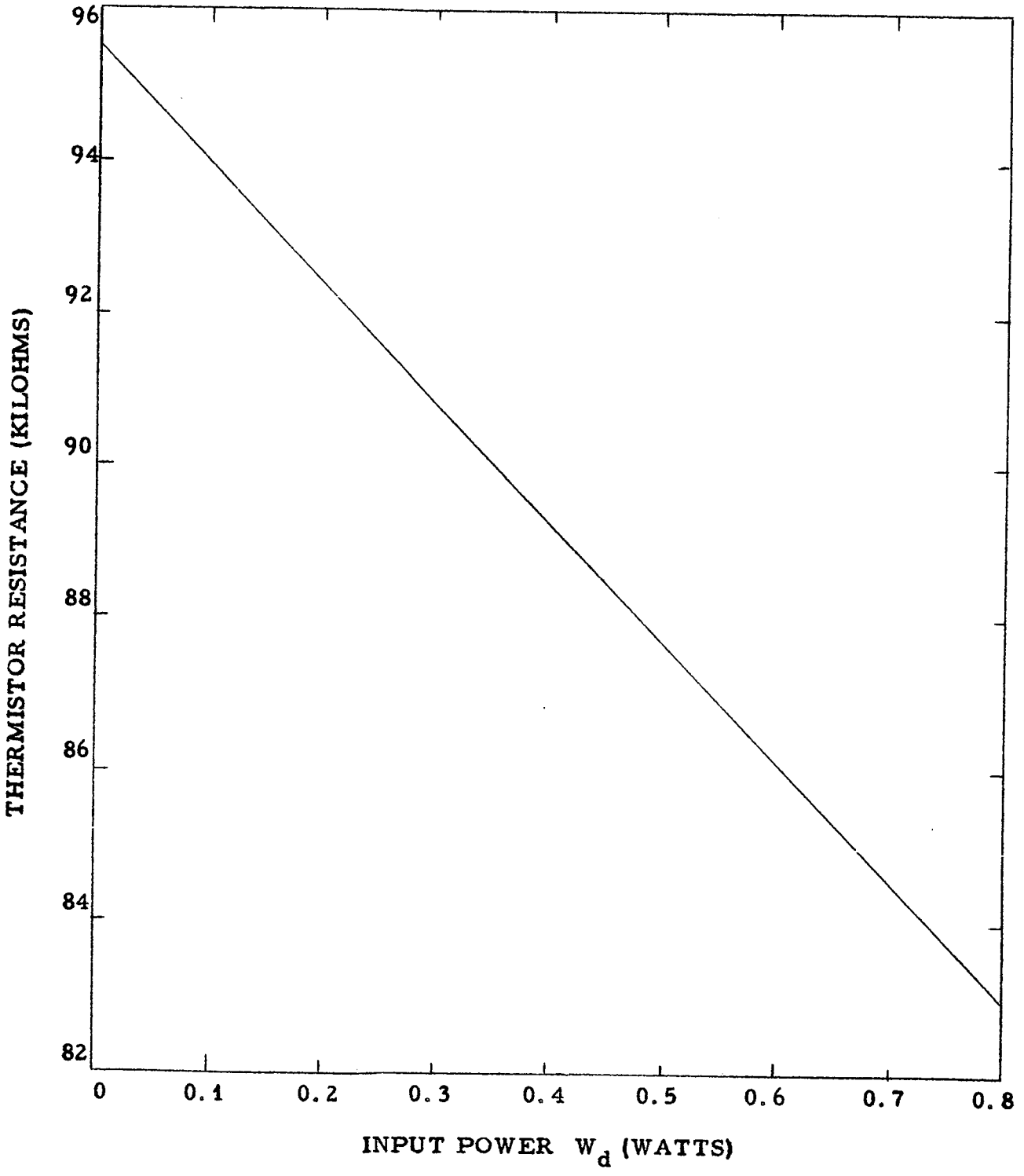

Figure 23. Calibration data for calorimeter.

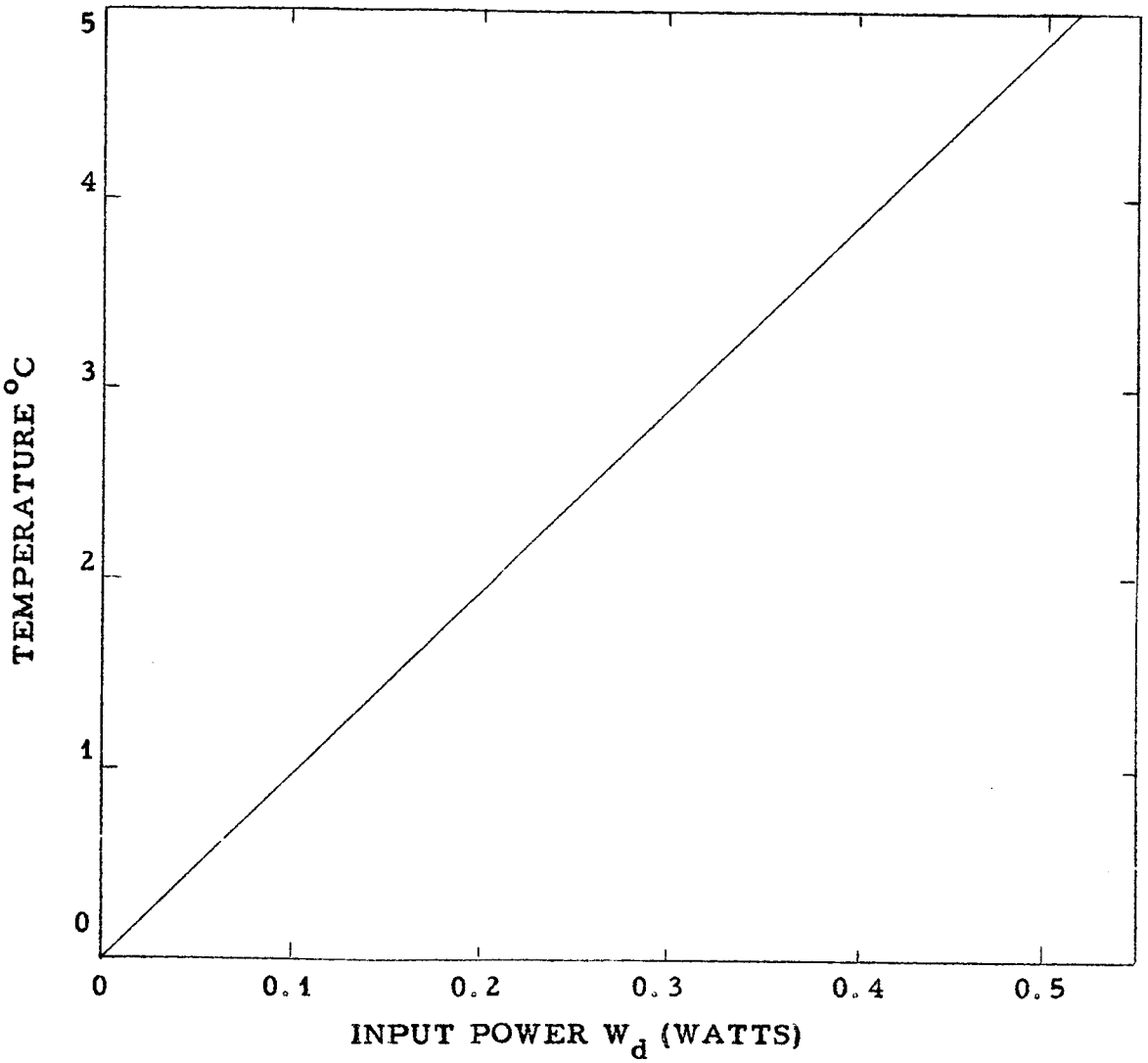

Figure 24. Specimen temperature as a function of input power, W_d. Heat sink temperature = 0°C.

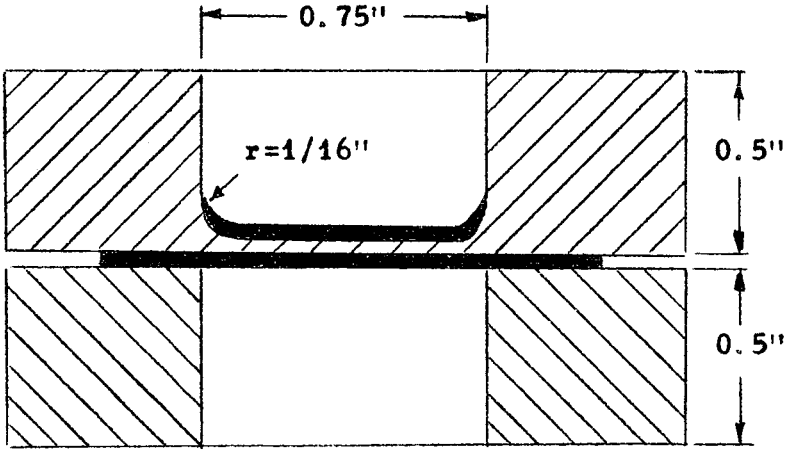

Figure 25. Cross-sectional view of calorimeter specimen.

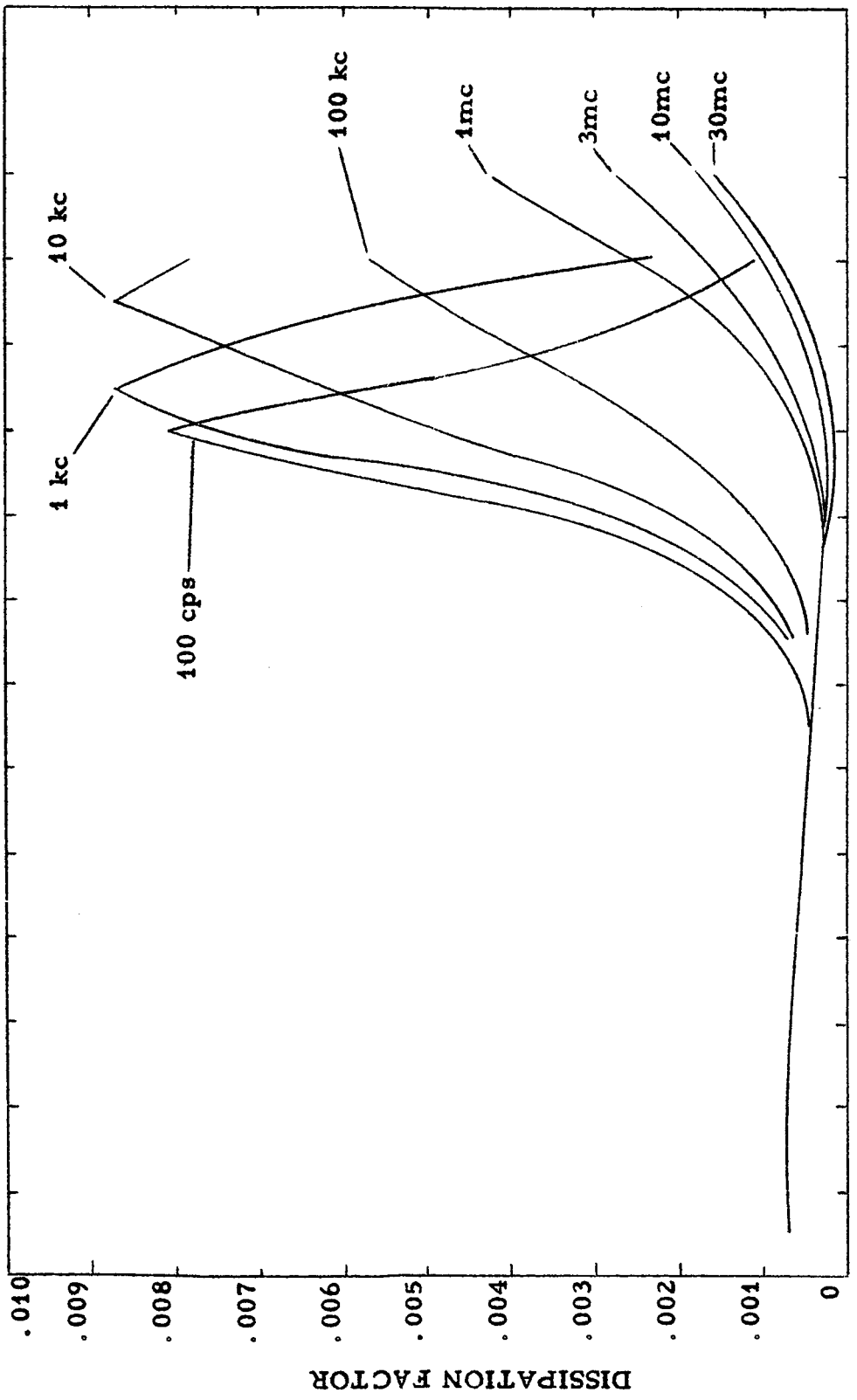

Figure 26. Effect of temperature on dissipation factor of C-1147. Rate of temperature rise 0.7°C per minute.

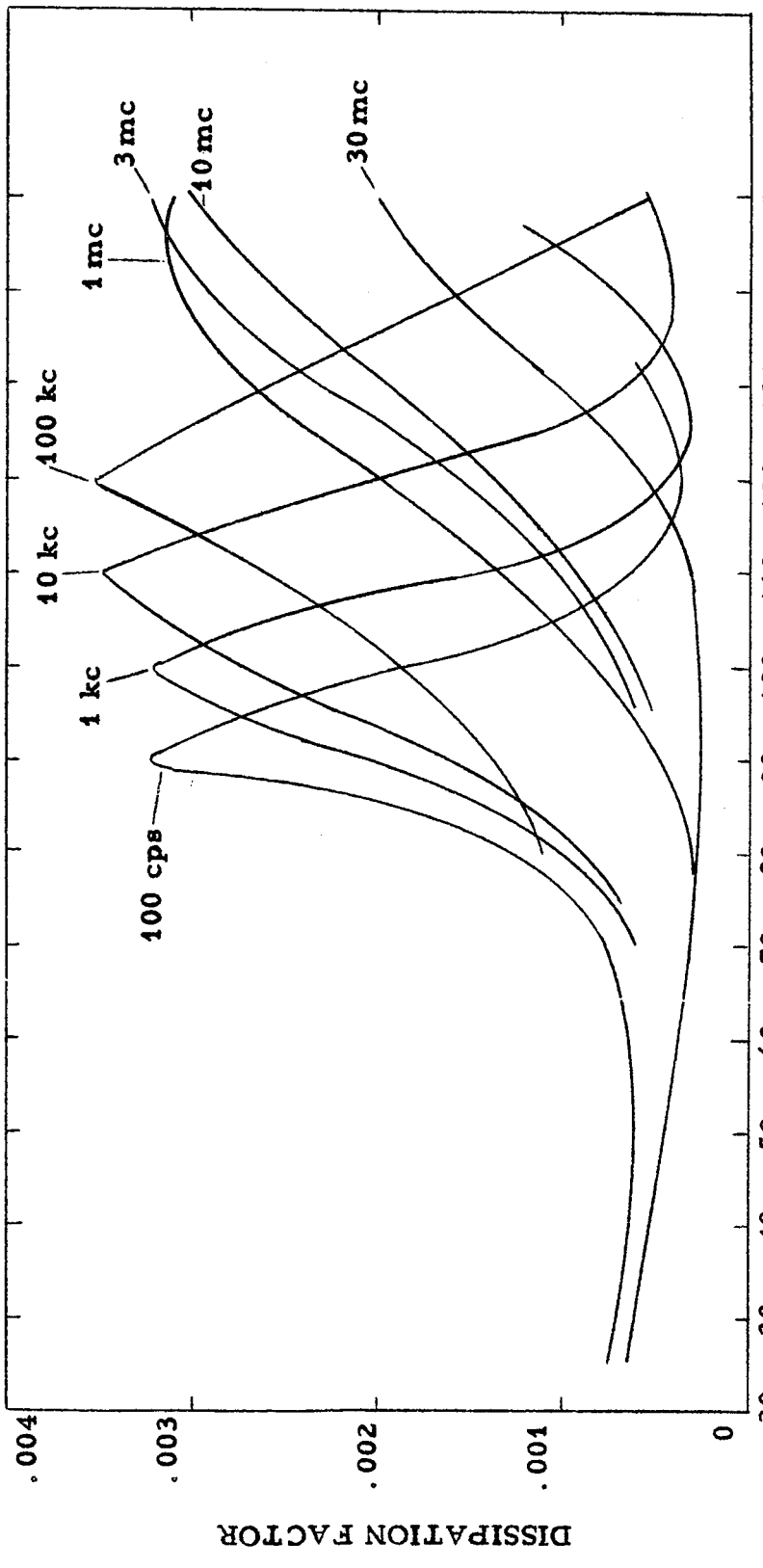

Figure 27. Effect of temperature on dissipation factor of Styron 666. Rate of temperature rise 0.7°C per minute.